Journal Code				Article ID					Dispatch: 05.12.18	CE: MAS
J	G	R	E	2	1	0	5	3	No. of Pages: 21	ME:

AGU100 ADVANCING EARTH AND SPACE SCIENCE

JGR

Journal of Geophysical Research: Planets

RESEARCH ARTICLE

10.1029/2018JE005681

Evolution of Escarpments, Pediments, and Plains in the Noachian Highlands of Mars

Jon C. Cawley[1] and Rossman P. Irwin III[1]

[1]Center for Earth and Planetary Studies, National Air and Space Museum, Smithsonian Institution, Washington, DC, USA

Key Points:
- Debris-mantled escarpments, regolith pediments, sloping aggradational surfaces, and depositional plains ~~formed~~ on Martian cratered terrain
- Noachian arid-zone geomorphology included aqueous weathering of basalt to fines, low-intensity fluvial erosion, and deposition in basins
- These processes smoothed and sealed Noachian ejecta blankets, which required little geomorphic work to form stable pediments

Correspondence to:
J. C. Cawley,
cawleyj@si.edu

Citation:
Cawley, J. C., & Irwin, R. P., III (2018). Evolution of escarpments, pediments, and plains in the Noachian highlands of Mars. *Journal of Geophysical Research: Planets*, *123*. https://doi.org/10.1029/2018JE005681

Received 21 MAY 2018
Accepted 19 NOV 2018
Accepted article online 24 NOV 2018

Author Contributions:
Conceptualization: Rossman P. Irwin III
Formal analysis: Jon C. Cawley
Funding acquisition: Rossman P. Irwin III
Investigation: Jon C. Cawley
Methodology: Rossman P. Irwin III
Supervision: Rossman P. Irwin III
Writing - original draft: Jon C. Cawley
Writing – review & editing: Rossman P. Irwin III

Abstract Extensive Noachian-aged intercrater planation surfaces comprise much of the southern highlands of Mars. We mapped aggradational and stable to degradational surfaces in three study areas with diverse relief elements and ages: the high and rugged relief of Libya Montes, the well-preserved intercrater plains of Noachis Terra, and the rolling relief with more drainage development in Terra Cimmeria. Here we describe four major geomorphic features that formed in these regions: debris-mantled escarpments, regolith pediments, sloping aggradational surfaces, and depositional plains. We interpret that with tectonic stability and an arid paleoclimate, these features supported slow pedogenesis, sediment transport, and diagenesis over hundreds of millions of years during heavy impact bombardment. Slow aqueous weathering generated primarily fine- or medium-grained particles from basaltic surfaces of impact ejecta and megabreccia. These sediments were collected in local lows, reducing surface roughness, permeability, and populations of small craters. Larger crater walls and structural escarpments retreated radially or linearly as ~5–20° slopes, indicating efficient removal of fine- or medium-grained debris but little downslope transport of coarse material by fluvial erosion or creep. Gently to moderately sloping, composite intercrater planation surfaces evolved as regolith pediments with tectonic stability and little fluvial dissection. Noachian impact craters degraded in place on pediments and became embayed or buried on basin floors. The concentration of aggradational surfaces in low-lying areas, lack of coarse-grained alluvial fans in most locations, and resistance to later eolian deflation suggest intermittent low-magnitude (hypo-)fluvial erosion with aqueous cementation or development of a lag in basins.

Plain Language Summary The surface of Mars at Libya Montes, Noachis Terra, and Terra Cimmeria includes steep eroded slopes, gently to moderately sloping stable surfaces, gently sloping low areas that were thinly buried, and flat-floored basins that accumulated thick deposits of sediment. The development of these surface features suggests low-intensity, intermittent erosion by running water and wind over hundreds of millions of years. The key elements of this landscape evolution include weathering of Martian basaltic bedrock to finer-grained sediments rather than coarse gravel, a lack of intense rainfall or snowmelt, minimal movement of loose material downslope, and processes that concentrated sediment in basins. The blankets of material ejected from impact craters required little erosion to form stable and better sealed surfaces, which were later eroded by rivers during brief wetter epochs of Martian history.

1. Introduction

1.1. Motivating Questions

Mars is unique among the planets and moons in having a geomorphic record of running water from the first billion years of solar system history. The widespread valley networks and overflowed lake basins in the Martian cratered highlands reflect an epoch of warmer and wetter conditions around the Noachian/Hesperian (N/H) boundary (e.g., Fassett & Head, 2008a, 2008b), or about 3.7 Ga (Hartmann & Neukum, 2001). The paleohydrology of rivers and lakes suggests runoff production up to ~1 cm/day during flood events and annual runoff production of ~0.1 times the annual evaporation from lakes (Irwin et al., 2005, 2015; Matsubara et al., 2013; Matsubara & Howard, 2009). In the UNESCO (1979) aridity index, these estimates correspond to semiarid conditions if 20–50% of precipitation drained into lakes or arid conditions at 50–100%. This environment must have been geologically short-lived, however, because prolonged erosion of this magnitude would have dissected and regraded the landscape to a much greater degree than is observed (Craddock et al., 2018; Pieri, 1980).

Before the incision of valley networks, Mars experienced a long epoch of impact crater degradation that does not occur in the present atmospheric regime (e.g., Craddock et al., 1997; Forsberg-Taylor et al., 2004). Crater walls retreated, the interiors filled with sediment and/or lava, and the surrounding ejecta blankets lost their original rugged morphology over hundreds of millions of years. This epoch of crater degradation through at least the Middle and Late Noachian Epochs was roughly 2 orders of magnitude longer (230 to 390 Myr; Werner & Tanaka, 2011) than the main epoch of valley development (potentially <1 Myr; Barnhart et al., 2009), implying a slow evolution of the Noachian landscape without much incision of fluvial valley networks. The Martian highlands also include hundreds of Early or pre-Noachian enclosed basins that are variably buried by ejecta from the Hellas, Idisis, and Argyre impact basins (Frey, 2006). These ancient buried basins do not appear to have ever overflowed, at least since the Hellas impact, suggesting that potential evaporation was much higher than precipitation on Noachian Mars (Irwin et al., 2011).

The apparent long-term aridity and tectonic stability of Noachian Mars (e.g., Irwin & Watters, 2010; Phillips et al., 2001) allowed expansive planation surfaces to develop in the highlands. Planation surfaces are defined as large-scale surfaces with low relief and little fluvial dissection that generally crosscut bedrock structures (e.g., Migoń, 2004). As metastable features, intercrater plains typically have been presented as background canvas upon which later, more active geomorphic processes made their mark. The physical characteristics of these intercrater planation surfaces, however, place important constraints on the ambient Noachian environment. Hydrologic techniques based on paleochannel geometry or mass and energy balance in paleolakes are not applicable to the Noachian Period, because small (<2–4 km in diameter) impact craters and fluvial depositional landforms are not well preserved from that time (Hartmann, 2005; Irwin et al., 2013). Impact crater populations, degraded crater morphology, intercrater planation surfaces, and outcrops of weathered material have provided much of the basis for interpreting Middle to Late Noachian resurfacing in the literature. These features indicate that much more crater loss, crater degradation, resurfacing, and aqueous alteration occurred during the Noachian Period than afterward (e.g., Forsberg-Taylor et al., 2004; Hartmann & Neukum, 2001; Murchie et al., 2009; Tanaka et al., 1988), albeit at a lower rate than is observed in most regions on Earth (Craddock et al., 1997).

Here we focus on three basic questions regarding intercrater planation surfaces:

1. Did they evolve over the full length of the Middle and Late Noachian Epochs, perhaps in equilibrium with the Noachian paleoclimate, or do they represent a brief resurfacing event with little subsequent modification? A long timescale would suggest a more stable paleoclimate and suite of geomorphic processes, relative to a short epoch of resurfacing.
2. Low-relief deposits buried or embayed impact craters on basin floors, but are the moderately sloping intercrater surfaces primarily erosional or depositional? Impact craters are tectonically stable landforms with well-constrained initial geometry, so we can use them to determine if intercrater surfaces experienced widespread aggradation (e.g., through airfall mantling), stability, or denudation (e.g., through fluvial erosion).
3. What geologic processes shaped the intercrater planation surfaces? Previous maps and other studies of intercrater plains have suggested that they reflect mare-type basaltic lava flows, widespread eolian mantling, or burial by big-basin ejecta (Malin, 1976; Scott et al., 1986), all of which involve net aggradation. Another possibility is that some intercrater areas are stable or erosional surfaces, in which case they would be thinly and incompletely mantled by debris. We also consider how fine- to medium-grained sediment could become concentrated in basins, resistant to eolian deflation, and nearly flat lying.

1.2. Previous Work

Early comparative studies in planetary geomorphology focused on impact craters and intercrater plains on the Moon, Mercury, and Mars (e.g., Leake, 1982; Oberbeck et al., 1977; Wilhelms, 1974). Observations showed that Martian craters had been degraded and/or obliterated to a larger degree than lunar or Mercurian craters (Hartmann, 1973; Malin & Dzurisin, 1977). These differences indicate more horizontal material transport in early Martian landscape evolution, as found by studies of Mariner 4 (Sharp, 1968), Mariner 6/7 (Murray et al., 1971), Mariner 9 (Malin, 1976), Viking (e.g., Craddock et al., 1997), and subsequent data sets (e.g., Mangold et al., 2012). Based on early computer models, Chapman (1974) and Jones (1974) suggested that periods of increased geologic activity might have geomorphically altered Martian craters, but Hartmann (1973) interpreted that degradation had occurred at a more constant rate in the distant past. Later studies strongly supported long-term Noachian crater degradation rather than a brief erosional or depositional event, based on the wide diameter range of similar degradation states and the advanced degradation of stratigraphically older craters relative to younger ones of the same size (Craddock & Maxwell, 1990, 1993; also see Carr, 1981, p. 60).

Periglacial, eolian, fluvial, volcanic, impact, and mass wasting processes have modified Martian impact craters, but the relative effects of these processes have varied in space and time. Amazonian periglacial "terrain softening" is prevalent at latitudes >30–40° (e.g., Jankowski & Squyres, 1992), but apparently not in the equatorial region (e.g., Kreslavsky & Head, 2003). Eolian mantling has modified craters in the equatorial Arabia Terra and Meridiani Planum regions, as well as along parts of the crustal dichotomy boundary (e.g., Barlow, 1995; Grant & Schultz, 1993; Kite et al., 2013; Mittlefehldt et al., 2018). These processes had less effect in other parts of the equatorial highlands, where studies of crater topography have indicated a dominant role for fluvial erosion in Noachian crater degradation (e.g., Craddock et al., 1997; Forsberg-Taylor et al., 2004; Howard, 2007).

A possible role for permafrost in modifying cratered surfaces and the occurrence of cold but briny melt waters (e.g., Fairén, 2010) ~~similarly~~ have been explored. Because of the contrast between softened craters with strong periglacial modification in the higher latitudes and the steep crater walls that were maintained in the equatorial region, this paper concentrates on how Noachian aqueous weathering and fluvial erosion may have differed from norms on Earth, and we do not specifically test whether the ground was frozen ~~all or part of the time~~.

Low-viscosity lava flows have resurfaced some crater floors (e.g., Gusev crater as described by Arvidson et al., 2006), but the extent of this flooding is debated on the basis of crater floor morphology and spectroscopy (e.g., Edwards et al., 2014; Irwin et al., 2018; Rogers et al., 2018).

Carr (1981) observed that intercrater plains are "intrinsically difficult to interpret" because their surfaces have been reworked through time, removing most diagnostic landforms. The Mariner and Viking imaging systems posed additional limitations. Using Mariners 6 and 7 images, Murray et al. (1971) noted that intercrater areas were much smoother in Martian cratered terrains than in the lunar highlands and that the crater rims and ejecta were more subdued. These observations implied that Mars had undergone more leveling and lateral transport of surface material. If the transport process was eolian, then effective weathering was required to reduce hundreds of meters or kilometers of rock to small, transportable grain sizes. Chapman et al. (1969) and Cintala et al. (1976) had suggested ballistically emplaced or base-surge impact deposits as possible alternative processes. Wilhelms (1974) favored lava flows for some lightly cratered plains, based on ridges, flow fronts, and embayment relationships like those seen in the lunar maria.

Malin's (1976) thesis included the most thorough discussion of Martian intercrater plains to date. Based on Mariner 9 imaging, he interpreted intercrater plains as "stratified consolidated and unconsolidated materials, probably loose debris blankets and volcanic flows." The unconsolidated material was interpreted as impact and eolian materials (see also Chapman et al., 1969), which were more susceptible to erosion, fluvial incision, and development of chaotic and fretted terrains than was consolidated rock. He identified stratification in a variety of geologic settings (some of which might not be described as intercrater plains today), where secondary processes had formed escarpments, exposing layers in the older materials.

Malin and Edgett (2001) confirmed with the Mars Orbiter Camera (MOC) "that nearly everywhere that the subsurface of the Martian cratered highlands [is] exposed, the upper crust is layered." They favored long-term crustal evolution with concurrent impact cratering, erosion, and deposition forming a pervasively layered crust, as opposed to an initially Moon-like megabreccia with superimposed patches of fluvial and eolian deposits. Bandfield et al. (2013) developed a similar concept for aggradation of poorly consolidated fine-grained particles in the Noachian highlands, favoring a volcaniclastic source.

The Mars Exploration Rover (MER) Spirit's investigation of the Columbia Hills in Gusev crater found multiple generations of draping by impactites and volcaniclastic material that experienced subsequent aqueous infiltration, cementation, and alteration (Crumpler et al., ~~2015~~; McCoy et al., 2008; Squyres et al., 2006). The MER Q6 Opportunity showed that the eroded rim of ~~Endeavor~~ crater has a draped airfall deposit that predates the extensive accumulation and alteration of eolian basaltic sand in the region (Mittlefehldt et al., 2018). Such airfall and eolian materials may have contributed to crater infilling ~~and intercrater mantling elsewhere, but the effects may be too old or on a scale too small to be resolvable from orbit~~.

In their 1:25,000,000 scale geologic map based on Mariner 9 data, Scott and Carr (1978) divided most of the Martian highlands into older, rugged "hilly and cratered material" and younger "cratered plateau material."

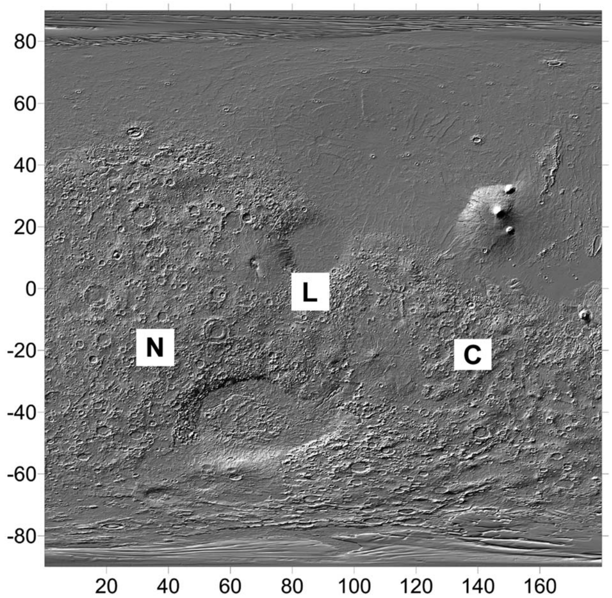

Figure 1. Mars Orbiter Laser Altimeter shaded relief map of the eastern hemisphere of Mars, showing the locations of study areas Noachis Terra (N), Libya Montes (L), and Terra Cimmeria (C).

The latter had flat, smooth intercrater plains with many buried to partly buried large craters. Secondary features including valleys, chaotic terrain, lobate scarps, and grabens also were present in the cratered plateau material. Scott and Carr (1978) interpreted the intercrater plains as due to widespread flooding by lava, leaving most of the craters exposed.

Scott et al. (1986) used a different subdivision of Noachian highland units based on Viking Orbiter imaging: hilly, cratered, subdued cratered, dissected, etched, and ridged units. In this scheme, the first three units are roughly comparable to the two Mariner 9 highland units, whereas the last three included areas of major secondary modification by water, wind, and tectonics, respectively. The mountain, basin rim, crater, and smooth plains units were similar between the Mariner- and Viking-based global geologic maps.

The most recent global geologic map of Mars used base data from the Mars Global Surveyor Mars Orbiter Laser Altimeter and Mars Odyssey Thermal Emission Imaging System (Tanaka et al., 2014). It does not define highland units based on secondary landforms, such as ridges, valleys, or etched terrain. Instead, it distinguishes rugged, high-relief outcrops of the Early Noachian highland unit (eNh) from the uneven to rolling, often visibly layered Middle Noachian highland unit (mNh) and the plains-forming Late Noachian highland unit (lNh). Irwin et al. (2013) found crater populations near saturation from 32- to 128-km diameters on the high-standing eNh unit, whereas the mNh unit was resurfaced around ~4 Ga, and the lNh unit includes later Noachian burial of basin floors. Noachian cratered terrain experienced more resurfacing at lower elevations, implying a gravity-dependent transport and/or deposition process.

Although the eNh and mNh units do not correspond exactly to the hilly and cratered and the cratered plateau units, respectively, of Scott and Carr (1978), the new global map recognizes both rugged highland terrain and intercrater planation surfaces. The new contacts are based on morphology, but the units are named based on their geologic province and crater densities, which are distinct for the highland units in diameter bins >16 km.

2. Methods

2.1. Selection of Study Areas

We selected three study areas (Figure 1) to encompass diverse relief, crater density, and fluvial dissection. F1

The Noachis Terra study area (13–25°S, 30–42°E; Figure 2) is densely cratered but less dissected by valley networks than the other two (Carr, 1995; Hynek et al., 2010), providing a more pristine view of older Noachian geomorphic surfaces. It includes Early Noachian upland terrain and intercrater planation surfaces in the high-standing Hellas basin annulus (Smith et al., 1999). The linear tectonic escarpments that bound Hellas-concentric grabens in this area (Wichman & Schultz, 1989) provide a useful comparison to impact crater walls and basin rim massifs for observations regarding scarp retreat. Gentle intercrater slopes of $<1.5°$comprise most of the study area (throughout the paper, we describe slopes of $<1.5°$ or 0.026 as gently sloping, 1.5–5° as moderately sloping, and $>5°$ or 0.087 as steeply sloping). F2

The Libya Montes study area (5°N–7°S, 80–92°E; Figure 3) has many rim massifs, intermontane planation surfaces, and incompletely filled structural basins around the Early to Middle Noachian Isidis basin (Irwin et al., 2013; Werner, 2008). The northern part of this study area has longer integrated surfaces descending into Isidis basin, whereas areas to the south are multibasinal. The high and rugged relief in this landscape supports a comparison with more densely cratered landscapes in the other study areas. Crumpler and Tanaka (2003), Howard et al. (2005), and Bishop et al. (2013) previously mapped northern portions of this area. They identified relief features like those in our map, but they subdivided the mountainous and upland intercrater areas differently. Phyllosilicates are concentrated in the uplifted bedrock and overlain in swales by an olivine-rich unit and a pyroxene-bearing caprock (Bishop et al., 2013; see also F3

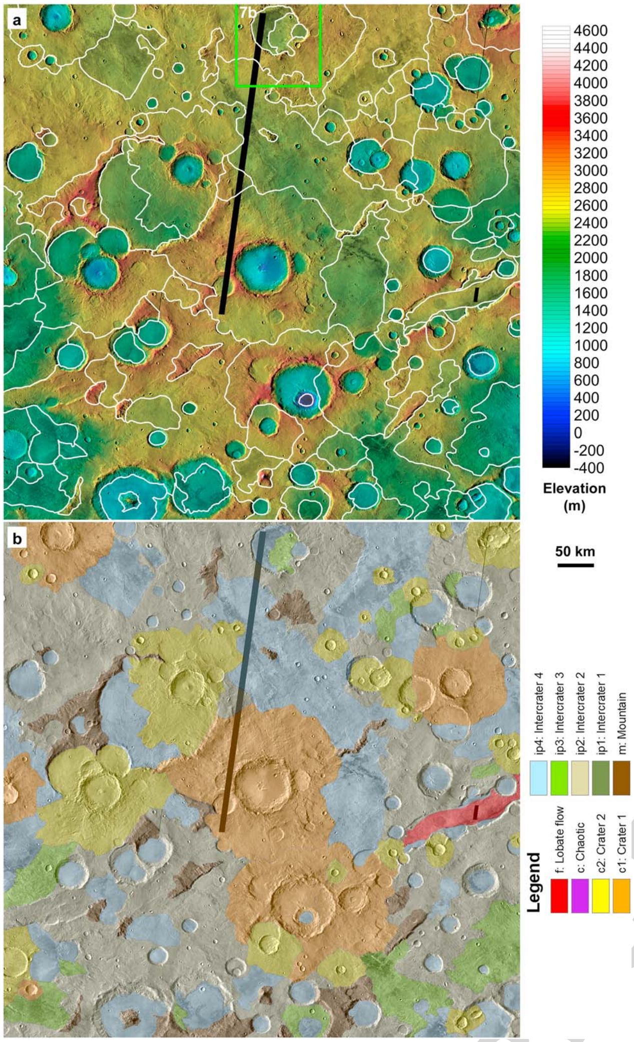

Figure 2. Noachis study area (13–25°S, 30–42°E). (a) Thermal Emission Imaging System daytime infrared mosaic colorized with Mars Orbiter Laser Altimeter topography, showing mapped contacts as white lines. The green box shows the location of Figure 7b. (b) Map of the study area. The SW-NE linear escarpments are normal faults circumferential to the Hellas impact basin (Wichman & Schultz, 1989).

Tornabene et al., 2008). Studies of the valley networks that incise these surfaces include those by Jaumann et al. (2010) and Erkeling et al. (2010).

The Terra Cimmeria study area (16–27°S, 132–144.5°E; Figure 4) contains mostly Early to Middle Noachian intercrater surfaces in the ejecta annulus northeast of Hellas basin. This area is more densely dissected by valley networks, and here it is useful to observe how Late Noachian to Early Hesperian ~~overland~~ flow responded to older intercrater topography. This study area is one of the sites reproduced in a simulation model by Matsubara et al. (2018). F4

2.2. Mapping Approach

We used ArcGIS 10.5 software to map the study areas at 1:2:000,000 scale on a base mosaic of 100 m/pixel Thermal Emission Imaging System daytime infrared images (Edwards et al., 2011). The Mars Global Surveyor Mars Orbiter Laser Altimeter Mission Experiment Gridded Data Record at ~463 m/pixel (128 pixels per degree; Smith et al., 2003) provided a topographic base for mapping and slope measurements. The initial line work included polyline shapefiles that were snapped and converted to polygons.

In the Tanaka et al. (2014) global geologic map, the contact between the eNh and mNh units was typically placed at a slope break between a more steeply sloping, higher-standing, heavily cratered terrain (unit eNh) and a gently sloping, less densely cratered surface below it (unit mNh). These units were distinguished from the lNh unit, which is mostly younger basin fill with sharply defined contacts. We used the same general approach, but we specifically mapped surfaces where the Noachian degraded craters were exposed or buried.

For each of the three study areas, we created an ArcGIS point shapefile of the Robbins and Hynek (2012a, 2012b) impact crater database, which contains 384,335 craters globally and is statistically complete down to 1 km in diameter. We determined the relative age of each study area by dividing its crater data into diameter bins of D–D × $2^{0.5}$ km, with both the count (N) and error bars (±$N^{0.5}$) normalized to an area of 10^6 km^2 (e.g., Hartmann, 2005). We plotted the binned crater counts on Hartmann (2005) isochrons to provide a characteristic age for each study area.

3. Results

3.1. Description of Map Units

The Mountain unit contains steep-sided massifs, mesas, and fault-bounded blocks, which are surrounded by the gently or moderately sloping Intercrater 1–4 units. Most of the associated escarpments have retreated as steep slopes in the 5–20° range, but the Mountain unit also contains areas of moderate slope on plateaus and in swales (Figure 5). Most of the Mountain unit contacts are concave-up slope breaks, some of which are less abrupt than others (Figure 5d). These are the stratigraphically oldest outcrops in the study areas; the crystallization age of the bedrock predates formation of the mesas and massifs as morphological features. Stratigraphic relations with the Hellas and Isidis impacts suggest an Early Noachian age of the Mountain unit at Noachis Terra and Terra Cimmeria, and an Early to Middle Noachian age at Libya Montes (Tanaka et al., 2014), with slow erosion through the remainder of the Noachian Period. F5

Mountain unit outcrops have small or absent plateaus at the highest elevations; where higher-standing surfaces are more extensive, we mapped the Intercrater 1 unit (Figure 6a). This gently to moderately sloping unit has an Early to Middle Noachian age in Libya Montes, where it was resurfaced by Isidis basin ejecta, and in F6

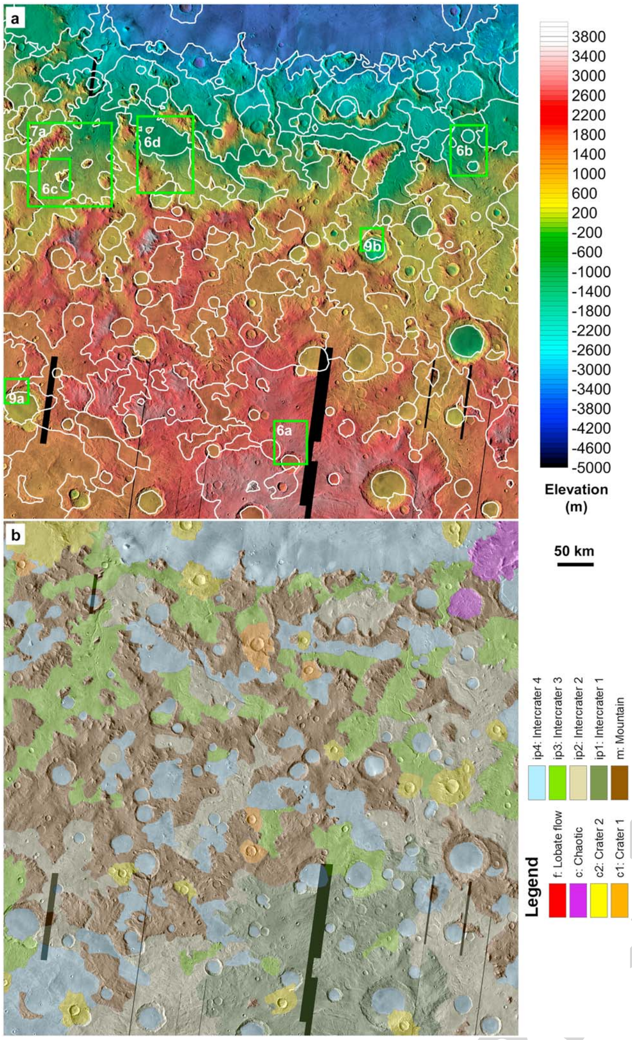

Figure 3. Libya Montes study area (5°N–7°S, 80–92°E). (a) Thermal Emission Imaging System daytime infrared mosaic colorized with Mars Orbiter Laser Altimeter topography, showing mapped contacts as white lines. The green boxes show the locations of subsequent figures. (b) Map of the study area.

Terra Cimmeria, where the outcrops include higher plateaus and ejecta of several post-Hellas degraded craters. This unit does not occur in the Noachis study area. As the highest-standing planation surface in the study areas, the Intercrater 1 unit has few sources for allogenic sediment, aside from ejecta and airfall material.

The Intercrater 2 unit (Figure 6b) is intermediate in age and topographic position. These outcrops are gently to moderately sloping and are transitional between the upland Mountain or Intercrater 1 and downgradient Intercrater 3 or 4 surfaces. The Intercrater 2 unit experienced the same loss of small craters as the rest of the study areas, but it does not have significantly exhumed or buried large craters, suggesting relative topographic stability through the Noachian Period. It is a composite surface: Local lows within the unit were a sink for upland sediments, but much of it was erosional, contributing material to Intercrater 3 and 4 surfaces downslope.

The Intercrater 3 unit (Figure 6c) was an aggradational down-gradient extension of Intercrater 2 surfaces through the Middle and Late Noachian Epochs. Most of it is gently sloping, with a lower occurrence of moderate 1.5–5° slopes relative to the Intercrater 1 and 2 units (Figure 5). Small craters and most larger craters were filled and buried there. It includes the lower reaches of some Noachian watersheds, as well as Noachian ejecta blankets that buried parts of basin floors (Figures 7a and 7b). The Intercrater 3 unit has a unidirectional gradient that allowed it to become locally dissected around the N/H boundary, contributing some sediment to Intercrater 4 basin fill.

The Intercrater 4 unit (Figure 6d) is confined to basin floors and is nearly flat or gently sloping inward. It is defined by pervasively buried or embayed Noachian craters, which require thick burial in the Noachian Period and Early Hesperian Epoch. The Intercrater 4 unit was the eventual sink for materials eroded from upslope areas, thus representing a primarily aggradational surface, and some basin floors may have experienced additional volcanic resurfacing (e.g., Goudge et al., 2012).

The youngest extensive units in the study areas are fresh impact craters and their ejecta. Some of these craters have visible fluvial dissection and related deposits (Crater 1 unit), whereas others do not (Crater 2 unit; Mangold et al., 2012). Where the ejecta blankets overlap, the dissected craters are older than the undissected ones. Mangold et al. (2012) found that dissected fresh craters north of Hellas and south of Margaritifer Terra have Early Hesperian to Early Amazonian ages (~3.7–3.3 Ga). We have excluded these craters and their ejecta from our analysis of the underlying planation surfaces.

3.2. Description of Study Areas

The Noachis Terra study area (Figure 2) includes small outcrops of the Mountain unit, most of which are aligned with Hellas-concentric normal faults or post-Hellas impact crater rims. Gentle to moderate Intercrater 2 slopes extend over much of this study area between the Mountain unit outcrops and Intercrater 4 basin floors. Aggradational Intercrater 3 surfaces include Noachian ejecta that overlie older basin fill, as well as other sloping deposits of unknown origin in various swales in the landscape (Figures 7a and 7b). Intercrater 4 deposits in Noachis are confined within impact craters and large intercrater basins; the latter are most extensive in the north-central portion of the study area. The significant aggradation in long swales suggests some locally integrated sediment transport along preexisting topographic features, but fluvial valley networks are not deeply incised here, and drainage is not well integrated. Sizable post-Noachian Craters 1 and 2 units cover significant portions of the terrain.

10.1029/2018JE005681

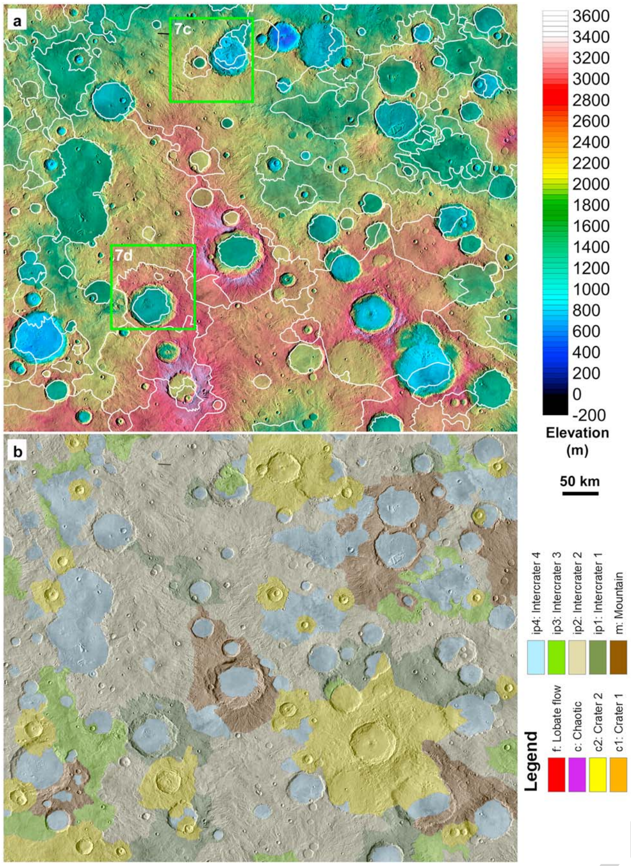

Figure 4. Terra Cimmeria study area (16–27°S, 132–144.5°E). (a) Thermal Emission Imaging System daytime infrared mosaic colorized with Mars Orbiter Laser Altimeter topography, showing mapped contacts as white lines. The green boxes show the locations of Figures 7c and 7d. (b) Map of the study area.

In contrast, the Libya Montes study area (Figure 3) has many high-relief Mountain unit outcrops along the Isidis basin rim. In general, the elevation decreases from the Intercrater 1 plateau in the south to the Isidis basin floor in the north. Drainage from south to north was poorly integrated through most of the Noachian Period. Most erosional Intercrater 2 surfaces are confined within structural valleys, which terminate in an Intercrater 4 deposit within an impact crater or a low part of the swale. Some of these surfaces may have originated as Isidis ejecta. The Intercrater 3 unit includes better integrated aggradational surfaces primarily to the north, which has a steeper regional gradient into the Isidis basin (Figure 3a). The development of valley networks around the N/H boundary was associated with overflow of enclosed structural and impact basins in Libya Montes, forming narrow breaches in former divides and dissecting older planation surfaces (Howard et al., 2005). It is worth noting, however, that much of the Noachian deposited sediment remains confined within structural basins upslope.

The Terra Cimmeria study area (Figure 4) includes the most pervasive post-Noachian fluvial overprint. Isolated Mountain and Intercrater 1 erosional surfaces are associated with older crater rims and Early Noachian impact-generated relief within the landscape. Intercrater 2 surfaces predominate the terrain, whereas aggradational Intercrater 3 slopes occur in smaller areas marginal to Intercrater 4 depositional basins. Ejecta blankets surrounding various Noachian craters are eroded back to form smaller escarpments and/or breaks in slope (Figures 5d, 7c, and 7d). Intercrater 4 deposition centers occur as discrete infilled craters and one sizeable infilled swale in the northwestern corner of the study area, associated with better developed fluvial valleys. Here also, later Crater 1 and 2 ejecta obscure a portion of the study area.

Using the Hartmann (2005) method, our crater counts (Figure 8) show a >4-Ga Early Noachian isochron age in Cimmeria and Noachis, approaching saturation at diameters >32 km. Libya has a younger surface corresponding to the Early to Middle Noachian Isidis impact at ~4 Ga (Irwin et al., 2013; Werner, 2008). All three study areas reflect a complete loss of Noachian primary and secondary craters at diameters <4 km. This resurfacing declined during the Early Hesperian Epoch (by about 3.5 Ga) in the study areas, consistent with previous findings at the global scale (e.g., Irwin et al., 2013).

4. Discussion

4.1. Debris-Mantled Escarpments

Escarpments are steep, laterally extensive slopes that separate two low-gradient surfaces above and below them. In our study areas on Mars, Noachian escarpments are debris-mantled slopes with sharp breaks in slope at the top and bottom, and little fluvial dissection in most cases. They occur on the walls of degraded impact craters, impact basin rim mountains, and tectonic faults, but Martian inselbergs would have experienced similar erosion of slopes. Scarp retreat processes formed more smoothly sloping interior walls from the original rugged slump terraces of complex impact craters. Highland escarpments developed mostly in impact ejecta or megabreccia (including the thick ejecta blankets of large basins), and most lie below the angle of repose. The interior walls of Noachian impact craters have declined in slope from an initial maximum of ~20–35° to ~10–20°, with some in the 5–10° range and few as high as 20–25° (Kreslavsky & Head, 2003; Mangold et al., 2012).

Relative to terrestrial analogs of similar size, Noachian escarpments on Mars retreated linearly (tectonic escarpments) or radially (crater wall escarpments) without becoming deeply dissected. This morphology is consistent with the overall reduction of high-frequency relief in the Noachian landscape through time. The ruggedness of escarpments varies between the more dissected (Cimmeria) and less dissected (Noachis)

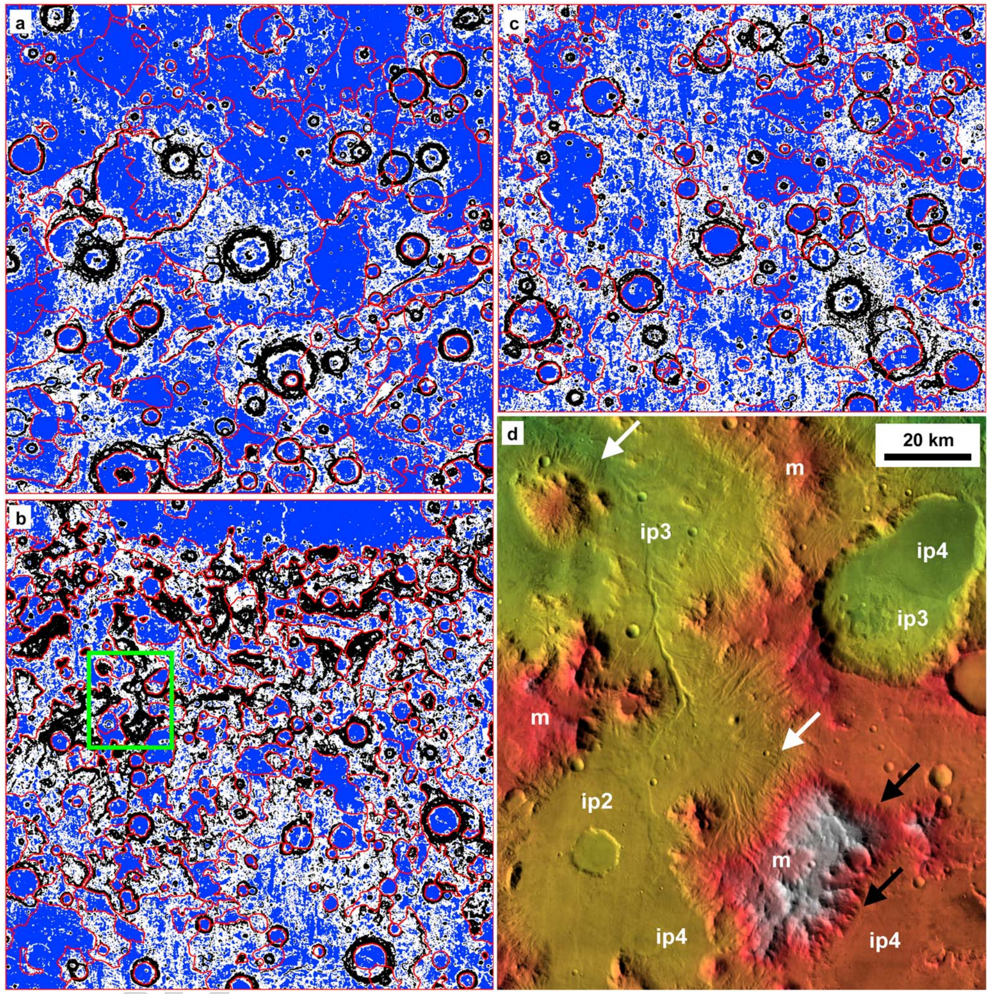

Figure 5. Maximum slope to the eight adjacent pixels for each 128 pixel per degree Mars Orbiter Laser Altimeter grid cell. Slopes are binned as gentle (<1.5°, blue), moderate (1.5–5°, white), and steep (>5°, black), as described in the text. Red lines are mapped contacts. Generally, solid blue areas are depositional plains, mixed areas are sloping aggradational surfaces and pediments, and black structural escarpments of impact origin bound the mountains. Many mountain unit outcrops contain plateau surfaces and swales of intermediate slope. (a) Noachis Terra, with gentle slopes over much of the area. (b) Libya Montes, with a green box showing the location of Figure 5d. (c) Terra Cimmeria. (d) Portion of the Libya Montes study area, showing example slope relations between degradational and aggradational units. Unit abbreviations are as in Figures 2–4, but mapped contacts are removed to more clearly show the surface features. The base of an escarpment can have either a sharp break in slope, usually at the contact with an aggradational unit (e.g., black arrows), or, less often, a more gradual ramp that may be an alluvial bajada (e.g., white arrows). Some escarpments are deeply dissected, but this is a localized occurrence that may be a Noachian/Hesperian boundary decoration on older slopes. The Intercrater 2 unit (ip2) contains Noachian impact ejecta that is to be more resistant to Noachian/Hesperian erosion than the underlying Intercrater 4 (ip4) material, such that the ejecta blanket now stands in relief.

regions, but the dense valley networks in Terra Cimmeria appear to be a N/H decoration on an older cratered landscape rather than a mature dendritic pattern (e.g., Pieri, 1980).

A lack of deep dissection and fan development along escarpments through most of the Noachian Period (Moore & Howard, 2005) suggests that either these slopes did not produce gravel efficiently or gravel was produced but not transported. In any event, very little material accumulated along the base of Noachian escarpments (Figure 9). The relaxation of these slopes by ~10–15° over ~10^8 year timescales during heavy **F9** bombardment (Mangold et al., 2012) indicates some movement of coarse materials, but creep driven by freeze-thaw, wetting-drying, or small impacts must have been remarkably slow to maintain such well-defined escarpments to the present. Kreslavsky and Head (2018) showed that Late Hesperian to Amazonian creep has strongly relaxed crater wall slopes at middle to high latitudes, but not around the equator, so equatorial

10.1029/2018JE005681

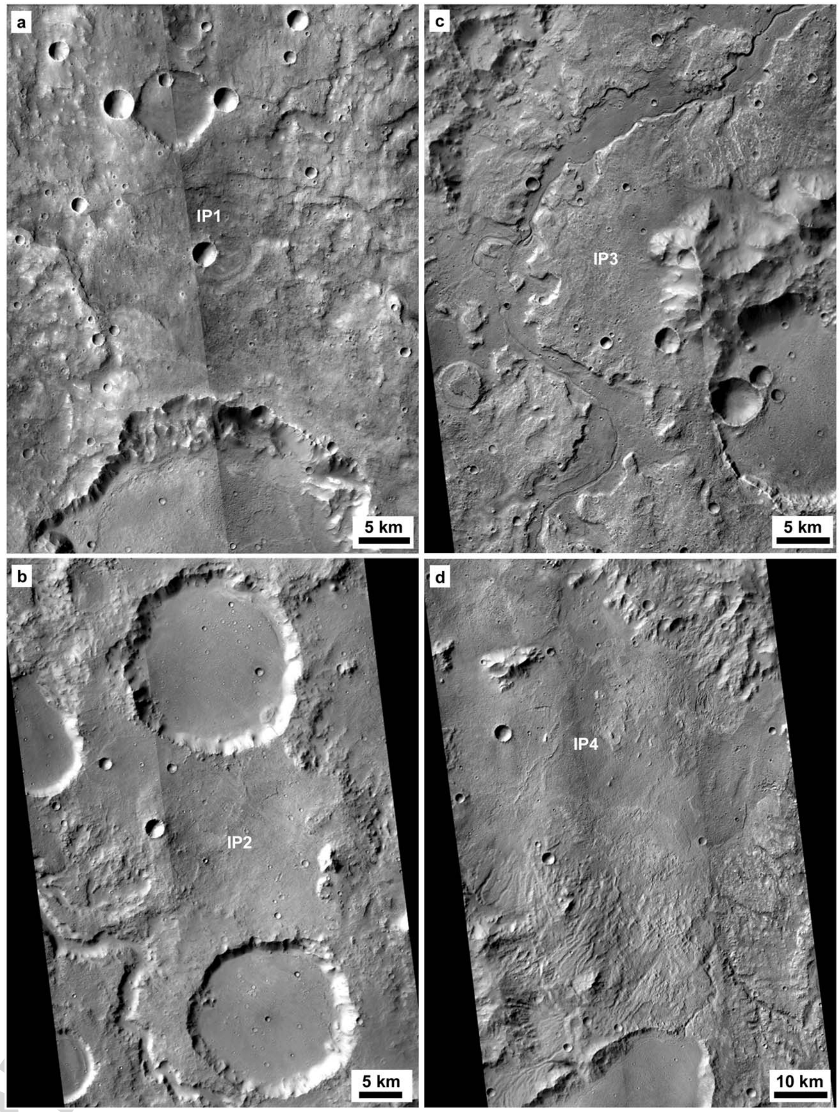

Figure 6. Example planation surfaces in the Libya Montes study area, seen in ~~CTX~~ imaging. The labels indicate representative outcrops, although each frame contains outcrops of other units as well. (a) Intercrater 1 unit (IP1) regolith pediment, centered at 5.2°S, 86.7°E. CTX J05_046719_1728 and D02_027849_1729. (b) Intercrater 2 unit (IP2) regolith pediment, centered at 1.6°N, 90.9°E. Note the exposed degraded craters. CTX P19_008386_1816 and P19_008531_1820. (c) Intercrater 3 unit (IP3) sloping aggradational surface, centered at 1.0°N, 81.2°E. Note the buried crater and susceptibility of the material to fluvial erosion, relative to the valley incised into IP2 in Figure 6b. CTX B19_017221_1804 and J01_045150_1812. (d) Intercrater 4 unit (IP4) depositional plains, centered at 1.7°N, 83.8°E. Note that all Noachian craters are buried in IP4. CTX P17_007793_1805, B02_010575_1812 and P20_008874_1822. See Figure 3 for locations and context. Q7

Noachian slope processes did not involve freezing and melting of ground ice of a similar magnitude. As we noted in section 1.2, limited freeze-thaw creep does not necessarily imply that the ground was thawed most of the time, only that it did not frequently freeze and thaw in the presence of water. Clifford (1997) argued that seismicity from large impacts may have reworked loose (potentially saturated) material through liquefaction, but if so, then Martian escarpments generally must not have been water laden. Notwithstanding the foregoing arguments, crater walls must retreat by 10–30% of the crater radius (e.g., 2.5–7.5 km of wall retreat in a 50 km crater) to explain the volume of infilling material if rock volume is conserved, indicating significant denudation of slopes over time (Craddock et al., 1997).

In eroded landscapes, sharply concave breaks in slope often reflect large differences in the energy needed to erode the surface materials (see review by Parsons et al., 2009). The debris-mantled escarpments in our study

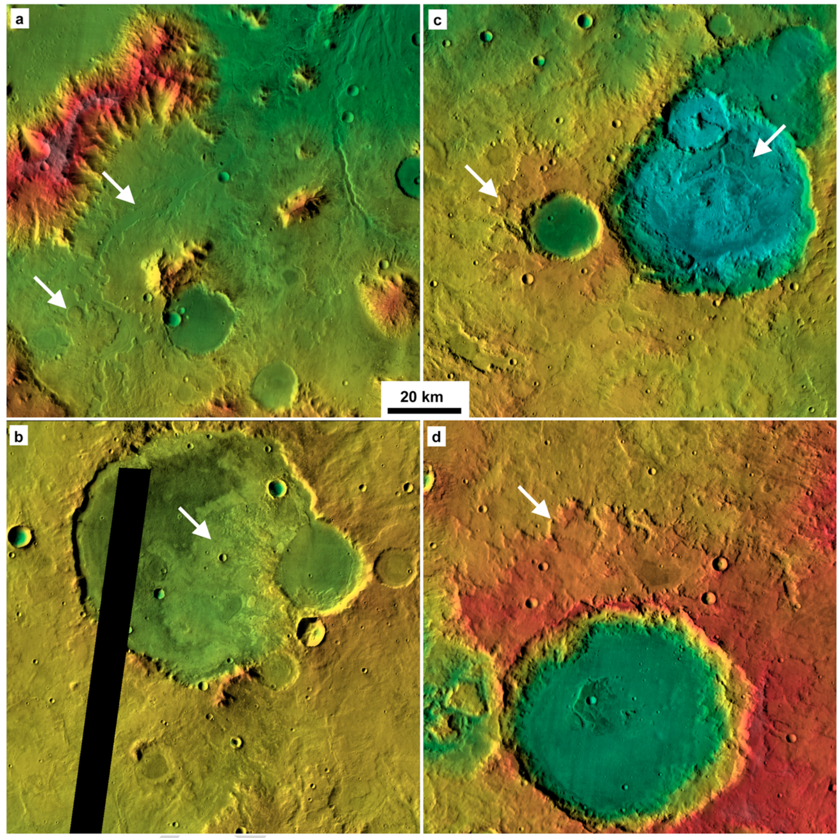

Figure 7. Examples of burial and erosion relations. (a) Intercrater 3 unit in Libya Montes, where a swale was infilled and later easily dissected, forming a wide valley (upper arrow) and leaving a circular feature in positive relief (lower arrow). See Figure 3a for the location and elevation coloring. (b) Intercrater 3 unit ejecta (arrow) from a 27-km crater deposited on the floor of an older 70-km crater in Noachis Terra. See Figure 2a for the location and elevation coloring. (c) Ejecta of 19-km (left arrow) and 17-km (right arrow) Noachian craters bounded by escarpments in Terra Cimmeria. (d) Ejecta of a 62-km crater in Terra Cimmeria bounded by an escarpment. These features suggest that resistant impact ejecta overlie less resistant material in these locations and/or that scarp retreat was not limited to primary structural escarpments on Mars. These examples also show that Noachian ejecta was not entirely removed by erosion, at least in some locations (also see unit ip2 in Figure 5d). See Figure 4a for the locations and elevation coloring of Figures 7c and 7d.

areas appear to be coarse grained, based on their resistance to eolian deflation (Figure 9). The sharp break in slope between a steep crater wall escarpment and a gently sloping floor deposit is consistent with a bimodal distribution of regolith grain size, with coarse basaltic debris on escarpments weathering to finer-grained sediment rather than to gravel (Allen & Conca, 1991; Dehouck et al., 2014), and the finer-grained sediments being deposited at low gradients on basin floors. In contrast, a more broadly concave break in slope would suggest a more continuous distribution of regolith grain size (Parsons et al., 2009). The sharp contrast between escarpments and low-gradient surfaces on Mars may reflect the efficient removal of weathered finer-grained debris from steep slopes, exposing the bedrock to further weathering and scarp retreat. Meanwhile, the inefficient removal of weathering products from low-gradient surfaces may have inhibited further weathering and denudation there.

Richter denudation slopes, which occur in alpine areas and Antarctica, are a morphological analog to Martian escarpments. These long, straight, poorly dissected slopes have a thin veneer of talus overlying a steep bedrock slope that follows the angle of the talus (Selby, 1993, pp. 366–368). The essential factors in maintaining Richter denudation slopes are uniform weathering and effective removal of the resulting debris under weathering-limited conditions. The lack of focused erosion at the top of the slope and deposition at the bottom allows the slope to persist rather than relax significantly over time, at least until the source of talus at the head of the slope is exhausted. In section 4.6 we discuss physical processes that might create a similar result on Mars, without necessarily implying a climatic analog to terrestrial Richter denudation slopes.

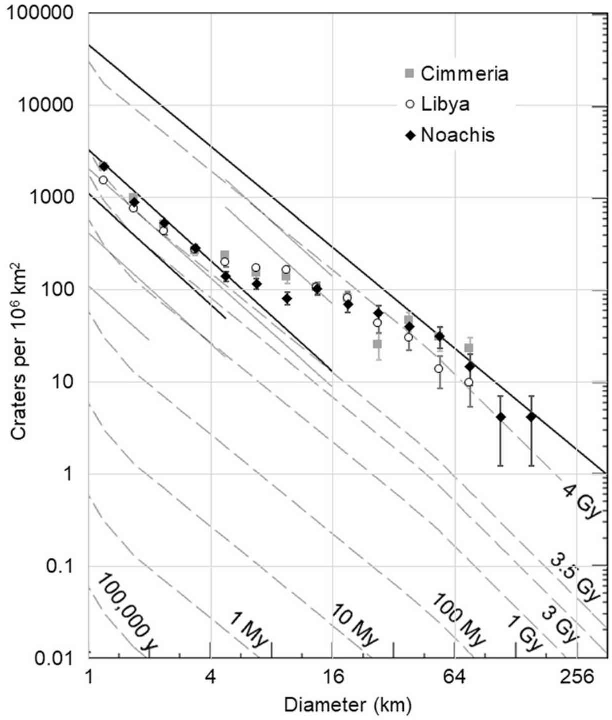

Figure 8. Crater counts from the Robbins and Hynek (2012a, 2012b) database, plotted on Hartmann (2005) dashed isochron lines for the Noachis (black diamonds), Libya (clear circles), and Cimmeria (gray squares) study areas. The Noachian/Hesperian and Hesperian/Amazonian boundaries defined by Tanaka (1986) are shown as solid lines. Error bars are shown but are smaller than the point symbols for some diameter bins.

4.2. Regolith Pediments

Pediments are gently to moderately sloping erosional surfaces of low relief, developed on bedrock or older unconsolidated deposits (Dohrenwend & Parsons, 2009). Surficial mantles of eroded sediment are thin and discontinuous (Cooke, 1970). Pediments may contain bedrock inselbergs and incised stream channels, but they are not densely dissected or undergoing rapid denudation.

Inclined, quasi-planar geomorphic surfaces can be aggradational (e.g., alluvial bajadas), but we find deeply buried impact craters only on the lower-lying Intercraters 3 and 4 units in our study areas, a strong indication that the outlying surfaces (Intercraters 1 and 2) were stable or degradational. Both pediments and bajadas convey sediment from upland source areas to downstream depocenters, and both may have concave longitudinal profiles (e.g., Blair & McPherson, 2009; Dohrenwend & Parsons, 2009; Strudley et al., 2006). The absence of deeply buried impact craters or deep fluvial dissection suggests an interpretation of the sloping Intercrater 2 planation surfaces as pediments, and on a larger scale, pediplains composed of coalesced pediments.

To contrast pediments from other types of planation surfaces, etchplains form by deep weathering of bedrock, followed by removal of the debris to expose the former weathering front (see review by Twidale, 2002). The traditional concept of a peneplain as a hypothetical late stage of prolonged fluvial erosion dates to Davis (1889, 1899), building on the earlier recognition by John Wesley Powell of base level control on fluvial erosion. Both etchplains and peneplains would involve more advanced weathering and fluvial erosion of the highlands than are evident in the orbital high-resolution imaging.

Nevertheless, weathering plays a significant role in the evolution of pediments, either on the present surface or under a previous regolith cover. Pediments are not relict alluvial plains; rather, they are erosional surfaces that crosscut the underlying bedrock or stratigraphy (although perhaps not deeply in some cases; Dohrenwend & Parsons, 2009). Many arid-zone pediments on Earth may have formed predominantly under past semiarid conditions (e.g., a precipitation to potential evapotranspiration ratio [P/E_p] of 0.2–0.5 in the UNESCO, 1979, scheme), where vegetation retained an alluvial cover that was lost in the present climate. The thin, discontinuous mantle of sediment leaves pediments exposed to physical and chemical weathering under arid conditions (P/E_p of 0.03–0.2 in the same scheme) as well (e.g., Amundson et al., 2008).

Twidale (2014) distinguished pediments that are thinly mantled by allochthonous transported sediment from those covered by autochthonous material that was weathered in place. Martian pediments may be a combination of both, with mixing of these materials and the regolith substrate by impacts (e.g., Oberbeck et al., 1977). In our study areas, pediments typically developed on a regolith of Noachian impact ejecta or megabreccia rather than bedrock.

The stability of regolith pediments over ~10^8-year timescales suggests that the geomorphic regime in the Noachian highlands was at or below thresholds for fluvial and eolian transport most of the time (i.e., erosion was weathering limited). Otherwise, it is hard to explain low denudation rates over hundreds of millions of years (Golombek et al., 2006). Some channelized fluvial flows are possible, but streams tended not to incise deeply, reflecting an inability to transport the imposed sediment load and attack the substrate. Potential causes include low rates of rainfall or snowmelt, high infiltration rates, a coarse-grained lag, or some combination, perhaps related to low or variable atmospheric pressures (Craddock & Lorenz, 2017). The former explanation is the most comprehensive, and ongoing cratering might have sustained infiltration or a lag against weathering, but we note that the intercrater plains are not densely cratered at small diameters. Occasional sheetwash, infiltration, dissolution, recrystallization, and chemical weathering would be physically plausible in this setting.

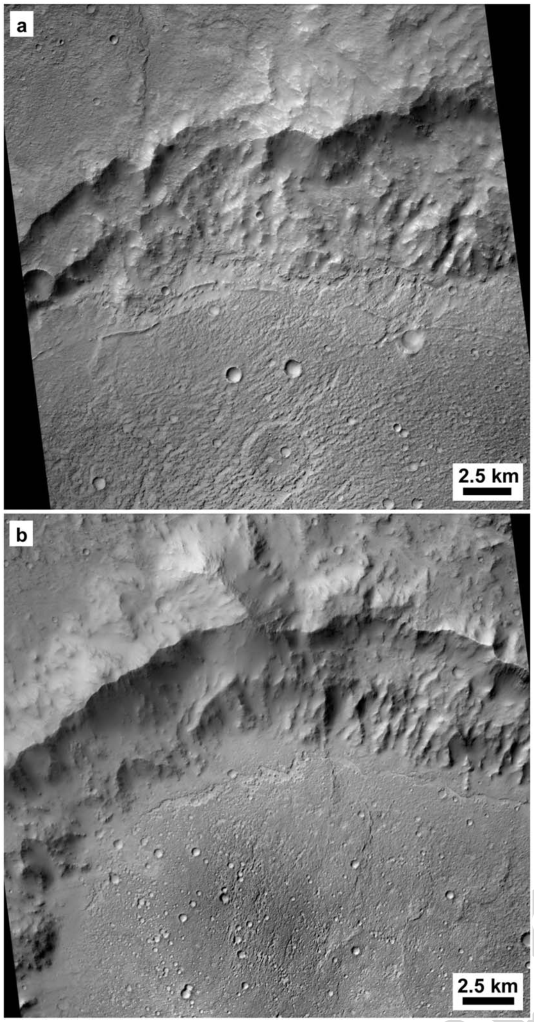

Figure 9. Example Noachian crater walls and floors in the Libya Montes study area. The original rims and slump terraces are partly degraded, but not deeply dissected. Much of the visible dissection may date to the epoch of valley network incision around the Noachian/Hesperian boundary. The crater walls are more resistant to wind than the etched surficial material on the crater floors. Little resistant coarse-grained material has accumulated at the base of the crater walls, leaving a sharp break in slope at the base of the walls. (a) CTX D21_035418_1747, centered at 4.0°S, 80.4°E. Note the circular feature at the bottom of the frame, a likely buried crater. (b) CTX P19_008452_1798, centered at 0.5°S, 88.6°E. See Figure 3 for locations and context.

Even in a weak fluvial regime on Noachian Mars, the lack of vegetation should have limited the accumulation of a thick sedimentary cover on uplands, leading to a sharp contrast between gently to moderately sloping erosional pediments underlain by regolith and flatter depositional plains with thick sedimentary fill. The sparse fluvial dissection with many local depositional centers (including small craters) suggests more locally than regionally integrated sediment transport pathways. The Martian highlands do not appear to have experienced integrated drainage until around the N/H transition, and then mainly on long preexisting slopes (Irwin et al., 2011).

Other observations suggest that the variable resistance of Martian stratigraphy may have controlled scarp retreat and the evolution of some highland pediments. Particularly in the more fluvially dissected Terra Cimmeria, some Noachian impact craters have an inclined Intercrater 1 planation surface outside their rims, bounded by a low escarpment that drops down to another planation surface at a lower level (Figures 7c and 7d). This morphology suggests that thicker and/or coarser ejecta close to a crater rim were more resistant than the underlying regolith, causing scarp retreat into strong-over-weak stratigraphy.

4.3. Sloping Aggradational Surfaces

Sloping aggradational surfaces on Mars are defined by a unidirectional gradient with mostly buried or eradicated Noachian craters. Some low-lying aggradational surfaces are ejecta blankets of adjacent Noachian degraded craters (Figures 7b and 7c), with $>1.5°$ gradients that are steeper than typical basin fill. Others are gently sloping buried swales in the lower reaches of integrated drainage, with no obvious source of contemporary crater ejecta (Figure 7a), suggesting a possible origin as an alluvial plain (Howard et al., 2005). Various channeling across their surfaces indicates that they transitioned to an erosional regime at some point in time, perhaps during the main epoch of valley development around the N/H boundary. Although they experienced net aggradation and lesser degradation at different points in time, the sloping aggradational surfaces occupied an intermediate position between stable to erosional surfaces upgradient and flat depositional plains downgradient for most of the Noachian Period.

4.4. Depositional Plains

The flat-floored morphology of Martian degraded craters was evident in Mariner flyby imaging (Sharp, 1968). Flat or gently inward-sloping plains ($<1.5°$) formed on crater floors, with a sharp break in slope separating them from the steeper crater walls (Craddock & Howard, 2002). These are low-relief surfaces with no prominent alluvial fans. Similarly, intercrater basins usually have sharp contacts between the basin floor and the surrounding upland surfaces, and their contributing N/H valley networks rarely have positive-relief terminal deposits (Malin & Edgett, 2003). These floor deposits are hundreds of meters to more than a kilometer thick (Forsberg-Taylor et al., 2004), such that even large craters of tens of kilometers in diameter became buried or embayed there. The lack of significant burial outside of basins suggests that sediment derived from upland escarpments and pediments preferentially accumulated in these long-term depositional centers. Lava flows also resurfaced some basin floors, like the Gusev crater floor that was investigated by the Spirit MER (e.g., Arvidson et al., 2006).

In a thicker early atmosphere, wind would have redistributed sand and fine-grained products of weathering on intercrater planation surfaces (e.g., Malin & Edgett, 2000), helping to fill and erase small craters or other irregularities in the landscape. This process occurs in very small craters today, for example, on the Gusev crater floor (Golombek et al., 2006). Silt and dust should be distributed widely by wind, including numerous dust devils, but we find no evidence for a thick, widespread eolian mantle in the study areas. The Mountain, Intercrater 1, and Intercrater 2 units show no evidence of deep burial in the past (e.g., thick and/or extensive fine-grained mantles, pedestal craters, or other erosional remnants). In this context, the wholesale burial of large impact craters on flat basin floors would require a separate mechanism for stabilizing sand and fine-grained sediments once they arrived in basins. Andrews-Hanna et al. (2010) argued that the location of sedimentary rock on Mars reflects where it was ultimately cemented, not where the sediments had been transported in the past. To explain the nearly flat-lying, laterally restricted deposits confined to basin floors, either the sediment transport process was gravity driven, the stabilization process was limited to basin floors, or some combination applied.

The first hypothesis is that sediment transport was dominantly fluvial, despite the limited dissection of intercrater pediments. We discuss fluvial erosion in more detail in section 4.6.

The second hypothesis involves a topographically restricted way to stabilize sediment. The simplest mechanisms are cementation or emplacement of a lag. In Gusev crater, Peace Class sedimentary rock is composed of sulfate-cemented grains of ultramafic sand (Squyres et al., 2006). The sulfate-cemented basaltic sandstone found by the Opportunity MER is the most compelling evidence of groundwater cementation on Mars to date (Landis et al., 2004). The hematite concretions in the same deposit are a lag-forming material that stabilizes the present surface against further deflation (Arvidson et al., 2004), having been concentrated on the surface by up to a few meters of prior deflation (Soderblom et al., 2004).

Original basaltic materials tend to weather in order of susceptibility, approximately: glass ~ olivine > plagioclase > pyroxene > opaque and refractory minerals (Eggleton et al., 1987; Salvatore et al., 2013). The specific alteration paths of basaltic materials differ with pH, as described by Tosca et al. (2004). Chemical weathering products of basalt include goethite, amorphous silica, iron smectite, and other clay minerals (Eggleton et al., 1987), any of which might be a useful stabilizing agent for sedimentary deposits. Geochemical studies by Chemtob et al. (2017) suggest that Noachian basalt weathering may have encouraged reduced iron smectites, whereas later oxidation would favor a transition to oxidized iron smectite and hematite. The presence of opaline silica at Gusev crater provides geochemical evidence of potential opal crust emplacement in Martian basaltic sediments (Milliken et al., 2008). Hydrated silica may play a more important part in Noachian pedogenesis and cementation than has been appreciated (Graham & Cawley, 2017; McLennan, 2003).

In any event, a hypothetical cementation process must have been strongly concentrated on basin floors, implying flow of surface water and/or groundwater rather than a spatially uniform process. Even in hyperarid regions ($P/E_p < 0.03$ in the UNESCO, 1979, scheme), the wetting of sedimentary deposits may be concentrated in basins, particularly if it involves surface water or groundwater that is sourced from higher elevations (e.g., in the Atacama Desert of northern Chile; Stoertz & Ericksen, 1974). In a low-energy geomorphic setting, the gentle inward slopes of most crater floors may reflect the gradient at which rain splash or sheetwash would rework surface materials before they became cemented.

As an alternative, a coarse-grained lag of fluvial sediments or ballistically emplaced material would be effective at armoring sedimentary fill (e.g., Howard et al., 2016), and it also would explain the flat floors. This alternative does not require a large fraction of coarse material, because lags are often a single grain in thickness and may be discontinuous (e.g., Cooke et al., 2006). Even in the thin Martian atmosphere of the Amazonian Period, saltating sand has moved granules and organized granule-coated eolian bedforms (e.g., Bridges et al., 2015), which may have played a significant role in stabilizing surfaces. Wells et al. (1995) showed that lags can accumulate eolian dust deposits beneath them, raising the lag surface on the order of ~1 cm/kyr. To explain the concentrated deposits on basin floors, however, a supporting process would have to remove similar dust deposits from the surrounding upland slopes.

Many basin floors have a mantle of Hesperian lava or basaltic sandstone (e.g., Edwards et al., 2014; Rogers et al., 2018), so it is important to note that the present surface may not reflect the Noachian stabilizing process.

4.5. Geologic and Tectonic Context

Mars has been a single-plate planet for most or all of its history, at least since the origin of the crustal dichotomy (e.g., Solomon, 1978; Watters et al., 2007), which is the oldest feature in the Martian geologic record (Irwin & Watters, 2010). Noachian intercrater planation surfaces formed over 10^8-year timescales in a metastable tectonic setting, where impacts were the main relief-forming process. Here we address two related issues: the applicability of a classic “geographical cycle” model of landscape evolution (Davis, 1899) in a landscape with no tectonic uplift and few drops in base level and the characteristics of impact craters that would limit incision of fluvial channels.

The science of geomorphology predates plate tectonic theory, and early concepts did not fully appreciate the dynamic nature of Earth’s surface, particularly near plate boundaries. The geographical cycle model of Davis (1899) involves a rapid orogeny followed by progressive erosion of a landscape to a low-relief late stage, termed a peneplain. This concept fell out of favor when clear examples were rarely if ever identified in the field (e.g., Daly, 1899). The cycle of uplift and erosion on early Mars is more like Davis (1899) described, however, because impacts are instantaneous events, and most of the landscape did not experience ongoing uplift.

The multibasin landscape of the Martian highlands has several major relief elements related to impact cratering, which are described here in order of declining scale. (1) The crustal dichotomy is the oldest and largest topographic feature on Mars, dating to the Early Noachian Epoch or pre-Noachian Period, depending on which stratigraphic timescale is used (Tanaka, 1986; Tanaka et al., 2014). (2) The basaltic crust of Mars was heavily impacted prior to about 3.8 Ga, leading to saturation of impact craters at ~40- to 90-km diameters in the oldest areas of the highlands (Irwin et al., 2013). (3) Ejecta from the Hellas, Isidis, and Argyre impact basins buried the pre-Noachian cratered terrain identified by Frey (2006) in the Early and Middle Noachian Epochs (e.g., Werner, 2008). These events left older buried basins with moderate interior slopes, in sharp contrast to the ~10–20° maximum interior wall slopes of typical of Middle and Late Noachian degraded craters (Mangold et al., 2012). (4) Numerous additional impact craters formed on these surfaces, so much of the exposed regolith was excavated from local craters rather than directly from Hellas or Isidis, but some of it is reworked Hellas and Isidis ejecta. (5) These later Noachian craters degraded in the manner described by Craddock et al. (1997), through scarp retreat and infilling.

As described by Forsberg-Taylor et al. (2004), the infilling of an impact crater reduces the relief of the crater wall and with it the contributing area for fluvial erosion of the wall. The interior wall slope also declines by ~10° (Mangold et al., 2012). In contrast to the Earth, where landscapes can be rejuvenated through tectonic uplift or various processes that change the base level for erosion, tectonically stable Mars had no mechanism to offset this negative feedback between crater wall erosion and the stream power of crater wall drainage as basins filled with sediment. For this reason, impact crater walls become less susceptible to fluvial erosion with time.

As a relief-forming process, impact cratering is not a highly effective way to rejuvenate landscapes. Impact craters are circular features that would radially disperse any flow generated from their exterior surfaces. Impact ejecta are initially permeable and have a concave-up radial profile that is reasonably graded for streamflow, providing little opportunity for deep incision of streams beyond the vicinity of the rim. The interior walls initially have high relief and steep slopes, but both decline over time (particularly the relief). If a crater wall retreated or the exterior surface aggraded or flooded such that water could overtop a crater rim, then the resulting base level drop could lead to dissection of the outlying surface. This situation was rare in the study areas, however, prior to the N/H boundary. Where older adjacent basins became integrated, it typically was through aggradation of one or both basin floors to bury the shared divide, rather than through overflow of water and incision of a narrow gap. These considerations imply that a cratered surface would require little geomorphic work to become a pediment.

In this light, the classic “geographical cycle” model of landscape evolution (Davis, 1899) pertains to Mars with respect to tectonic stability and eventual development of stable geomorphic surfaces. It differs from the terrestrial application, however, in that the initial conditions and paleoclimate did not encourage rapid erosion, so a stable end state was achievable without a lot of geomorphic work. The planation surfaces that we describe here are not peneplains in the traditional sense.

4.6. Aqueous Weathering and Hypo-Fluvial Erosion

Given the limitations imposed by tectonic stability and prevalent crater ejecta that would not generate runoff efficiently, it may not be surprising that the Noachian highlands are sparsely dissected. Valley networks did form over much of the planet around the N/H transition, however (e.g., Fassett & Head, 2008b), so the landscape could generate erosive runoff given an adequate water supply. Here we suggest that aqueous weathering and low-magnitude (hypo-)fluvial erosion may explain the aspects of scarp retreat, pedimentation, and basin infilling that are difficult to attribute to other physical processes during the remainder of the Noachian Period.

We focus our interpretation on fluvial erosion because other geomorphic processes would not produce the size range, age relationships, and rim morphology of degraded craters on Mars (e.g., Craddock et al., 1997; Craddock & Maxwell, 1990, 1993). Periglacial processes did not strongly modify equatorial highland craters, which maintained steep interior slopes during their degradation (e.g., Kreslavsky & Head, 2003). Volcanic infilling is particularly hard to reconcile with prolonged Noachian crater degradation, because of the need to sustain it (at least intermittently) and reproduce local relationships between the relative age and degradation of craters consistently on a global scale. Volcanic infilling also does not explain the degradation of crater rims. Mass wasting, including diffusion by small impacts, has modified craters on Mars and airless worlds (e.g., Craddock & Howard, 2000; Fassett and Thomson, 2014), but it is much less effective on plains than on slopes. Our mapped Intercraters 1 and 2 units represent cratered terrain that was never deeply buried, indicating a limited role for airfall mantling over time. The net infilling of basins and resurfacing of pediments, including the loss of all Noachian craters <4–8 km in diameter and extensive losses up to a few tens of kilometers (Irwin et al., 2013), require lateral redistribution of sediment.

On Earth, most of the geomorphic work accomplished by streams takes place during floods (Wolman & Miller, 1960). The erosion of headwater areas depends more strongly on larger floods (along with steeper slopes), because of the smaller contributing area and typically larger clast or block diameter of the substrate (Wohl, 2000, pp. 141–143). Where streams cannot transport the substrate material, the weathering rate limits the erosion rate (weathering-limited conditions). Where transportable material is abundant, but runoff is not, transport-limited conditions apply. A loose regolith may be weathering-limited under one set of conditions and transport-limited under another.

During the bulk of the Noachian Period, escarpments retreated, intercrater surfaces were smoothed, and sediment accumulated in basins, but there was little fluvial dissection. Around the N/H boundary, streams incised older intercrater surfaces to form valley networks, and hundreds of basins flooded and overflowed (Fassett & Head, 2008a). Howard et al. (2005) offered three possible explanations for the incision of valley networks: increased water supply, reduced sediment supply, or stabilization of the surface through development of a duricrust. We favor the former explanation, because it explains the contemporary paleolakes and is more straightforward to stop suddenly, for example, through freezing over a northern lowland sea. Duricrusts, however, may also have been an important contributing factor to both runoff production and sediment stabilization.

In a hypo-fluvial regime earlier in the Noachian Period, deposition of impact ejecta exceeded fluvial and eolian denudation, leading to the net aggradation of the highland intercrater surfaces that Matsubara et al. (2018) found when reproducing the topography of two study areas in a landscape evolution model (see also the Noachian craters with intact ejecta in Figures 5d, 7c, and 7d). These are transport-limited conditions in one sense, because the regolith could be transported if adequate runoff were available. Under the inferred Noachian arid or hyperarid conditions, however, coarse-grained regolith behaved as weathering-limited bedrock and developed stable pediments. The fine- or medium-grained products of chemical and mechanical weathering of basalt were preferentially removed and concentrated in basins. This concept predicts that most of the Noachian basin fill would consist of these products.

The lack of prominent deposits where most valley networks debouch into basins suggests that streams were transporting mostly sand and/or fine-grained sediment around the N/H boundary, that is, grain sizes that could be distributed across basin floors by unconfined flow or subsequently reworked by wind or waves. The apparent lack of adjustment of basin fill to N/H valley network activity suggests that the earlier sedimentary deposits were similarly fine or medium grained.

Thresholds for weathering and erosion would be very important factors in a hypo-fluvial regime, because the environment generally would not exceed those thresholds by wide margins. The following six progressive thresholds would be particularly significant. The water supply needed in each case would be lower in a cool desert than a warm one.

1. Adequate surface water to chemically weather basalt. This lowermost threshold is essential for Noachian crater degradation, which does not occur significantly in the present climate, and most of the highland surface is now stable over 10^9-year timescales. Above the weathering threshold, water may infiltrate a surface and subsequently evaporate, allowing dissolution, recrystallization, and/or ice fracturing in addition to chemical weathering. Desert varnish, opal and hyaline silica, or near-surface duricrusts may form (Channing & Butler, 2007; Graham & Cawley, 2017; Perry et al., 2006; Thiagarajan & Lee, 2004) at interfaces with fog, fine and intermittent rain, or condensation.
2. A small water supply that is not fully retained in a vadose zone, such that it maintains a deep water table but does not generate overland flow. Duricrusts, interstitial phyllosilicates, hydrated silica, and other secondary materials can form in these settings (Glotch et al., 2010). A water supply near these first two thresholds would be consistent with a hyperarid desert.
3. A water supply that exceeds the infiltration capacity during occasional events, generating sheet flow and perhaps some channelized flow, but no long-distance flow. This runoff could move fine- or medium-grained sediments and soluble materials downslope over time. Rain splash may be a feature of this level of water supply.
4. A water supply that exceeds the infiltration capacity by enough to transport sediment and incise channels. Recurring flow encourages weathering of the substrate and further channel incision. A water supply near thresholds 3 and 4 is common in terrestrial arid deserts.
5. A water supply of sufficient event magnitude and frequency to maintain small perennial lakes against evaporation and incise long channels or valleys. This threshold is exceeded in semiarid climates and apparently around the N/H boundary on Mars.
6. A water supply that exceeds the potential evaporation, such that many or all basins overflow, and the surface has fully integrated drainage. Mars does not appear to have ever exceeded this threshold.

In a low-energy hypo-fluvial regime, the long-term deterioration of resistance to erosion (e.g., weathering, comminution, and pedogenesis) can reduce the intrinsic thresholds for erosion, without needing to invoke large events with increased driving forces (Phillips, 1995; Ritter, 1988; Ritter et al., 2011). Under these conditions, the disintegration of surface material could occur while external variables remained essentially constant, with only gradual, often imperceptible, changes within the system (Schumm, 1973).

As an example, the weathering of basaltic bedrock to clay and accumulation of clay in the interstitial space within the regolith or in small basins would strongly reduce the magnitude of rainfall or snowmelt that is needed to generate ponding or overland flow. In terrestrial analogs such as arid tropical soils, illuviation and soil sealing by clays significantly limits further infiltration and increases potential surface flow (Amézketa Lizárraga et al., 2003; Ben-Hur & Lado, 2008). In terrestrial badlands, sealed lower alluvial surfaces can produce overland flow during rain events before adjacent upland escarpments, although fine materials erode far faster from unprotected escarpment surfaces when rain events continue further to soil saturation (Cerdà & García-Fayos, 1997).

Over the long term, water appears to have been the dominant erosional agent in our study areas, but precipitation must have been intermittent, of short duration, of low intensity, or some combination that would not deeply dissect the intercrater planation surfaces until around the N/H boundary. We see no indication that Mars ever experienced the kinds of strong storms that rain $>$10 cm in a day on Earth (e.g., deeply and densely dissected upland areas, lobate debris flows, or widespread coarse-grained deposits at the base of escarpments), even around the N/H boundary. We do not imply prolonged steady state conditions. Hypo-fluvial conditions would involve mostly surface wetting, infiltration, and sheet wash with minor channelized flow, like what is common on arid-zone terrestrial pediments. In this way, prominent features in the landscape would be preferentially exposed to weathering, and low areas would be filled and indurated, thus eliminating small-scale roughness features in the landscape without overdissecting it.

Fluvial erosion did not act alone. Fluvial erosion rates are higher at the base of an escarpment, where the contributing area is greater, than at the crest (Heimsath et al., 2006). This relationship has helped to maintain the steep terrestrial passive margin escarpments that have retreated ~1 km/Myr since the Jurassic to Paleogene breakup of Gondwana (Braun, 2018). Noachian crater wall retreat on Mars was more than an order of magnitude slower than these terrestrial examples (e.g., 2.5–7.5 km of retreat for a 50 km crater over ~10^8 Myr timescales, as discussed in section 4.1), and it occurred primarily during heavy bombardment.

We interpret scarp retreat on early Mars as the interaction of hypo-fluvial erosion as conceptualized here and a diffusive component (including small impacts), where water preferentially weathered and eroded the base of the slopes, and diffusive processes served to relax them (e.g., Craddock et al., 1997). Eolian reworking would be locally important as well, dependent on cementation processes that were concentrated in basins.

5. Conclusions

1. Pre-Noachian to Middle Noachian impact cratering, deposition of big-basin ejecta, and uplift of the Isidis rim established the macroscale topography of the highland intercrater planation surfaces in our three study areas. Subsequent erosion and deposition significantly reduced the microscale to mesoscale relief within the landscape but did not erase these regional foundations. Younger Noachian impact craters were degraded in proportion to their relative ages (e.g., Forsberg-Taylor et al., 2004), in many cases without being strongly buried or denuded, suggesting that the intercrater planation surfaces formed slowly over $>10^8$-year timescales during the Noachian Period.
2. Noachian geomorphic processes produced debris-mantled escarpments, regolith pediments (both of which were erosional surfaces), sloping aggradational surfaces, and flat depositional plains (both of which were depositional under nominal conditions). Gently to moderately sloping, relatively stable regolith pediments served as both erosion and transportation surfaces, whereas low-lying aggradational slopes and basin floors received sediments derived from the escarpments and pediments above. Some basins likely contain volcanic fill as well.
3. The concentration of aggradational surfaces in low-lying areas of the landscape indicates a gravity-driven erosional process and/or cementation mechanism, both of which are consistent with water. Crater degradation does not occur significantly in the study areas under the present atmosphere, and the reduction of crater rims requires active weathering in the past. Much of the weathering occurred below the threshold for channelized fluvial flow, because crater walls did not become deeply dissected. Occasional higher (above threshold) fluvial regimes may have achieved localized transport on regolith pediments and significant net transport downslope over long periods of time. Most surfaces did not experience deep fluvial dissection, suggesting that precipitation rates were low and very rarely exceeded threshold conditions for channelized flow or gullying. Slow scarp retreat also included a diffusive component, including from small impacts.
4. Eolian processes would have been more active under a thicker early atmosphere. Wind may have been responsible for the local reduction of microscale relief and some of the long-distance sediment transport into basins, but the lithification on basin floors implies flow of water and/or development of a topographically restricted lag.
5. Slow weathering of basalt to clay and iron oxides may have facilitated erosion in low-energy hypo-fluvial systems over extremely long periods of time. Soil sealing of interstitial regolith spaces by clay particles may have had significant effects in decreasing infiltration, increasing subsequent local erosion, and ponding, setting the stage for the N/H fluvial activity.
6. Development of coarse-grained, fluvially or ballistically emplaced lags, concretions or aqueous cementation may have stabilized fine- or medium-grained sediments in place on low-relief, low-lying depositional surfaces, limiting subsequent eolian deflation. The processes of stabilization were concentrated on basin floors, suggesting a role for flowing surface water or groundwater rather than regionally uniform wetting. Typical products of basalt weathering provide viable means to cement sedimentary deposits in basins.
7. Impact crater topography is radially dispersive in plan view, concave-up in cross section, and high in permeability, making it less susceptible to fluvial erosion. Cratered surfaces would require little geomorphic work to evolve into stable pediments.
8. The most deeply denuded parts of our study areas are the debris-mantled escarpments, which retreated linearly (tectonic scarps) or radially (crater walls) into adjacent uplands. The maintenance of maximum 10–20° slopes over ~10^8-yr timescales indicates very little creep related to freeze-thaw, wetting-drying, or other processes. We do not know whether the ground was frozen or thawed most of the time, but it did not frequently transition between the two in the presence of water. The lack of deep dissection of the escarpments or accumulation of alluvial fans at their base indicates that gravel was either not generated or not transported downslope in quantity. Martian escarpments are morphologically similar to

Richter denudation slopes, which maintain steep gradients over time through efficient removal of weathered debris, with little fluvial erosion or slope processes that would move coarse material and relax the slope.

Acknowledgments
The authors gratefully acknowledge the NASA Planetary Geology and Geophysics Program (Grant NNX14AN21G), as well as our colleagues Alan D. Howard and Robert A. Craddock, who have provided valuable input at several stages of this project. The Smithsonian Institution provided salary support to R.P.I. We thank Edwin Kite, Mikhail Kreslavsky, and an anonymous reviewer for their detailed comments that have improved the manuscript. ArcGIS shapefiles generated for this manuscript can be found at the Center for Earth and Planetary Studies (CEPS) data repository at https://airandspace.si.edu/research/data-repository.

References Q11

Allen, C. C., & Conca, J. L. (1991). Weathering of basaltic rocks under cold, arid conditions—Antarctica and Mars. *Proceedings of Lunar and Planetary Science*, *21*, 711–717.

Amézketa Lizárraga, E., Aragüés Lafarga, R., Carranza, R., & Urgel Cabrera, B. (2003). Chemical, spontaneous and mechanical dispersion of clays in arid-zone soils. *Spanish Journal of Agricultural Research*, *1*(4), 95–107. https://doi.org/10.5424/sjar/2003014-51

Amundson, R., Ewing, S., Dietrich, W., Sutter, B., Owen, J., Chadwick, O., & McKay, C. (2008). On the in situ aqueous alteration of soils on Mars. *Geochimica et Cosmochimica Acta*, *72*(15), 3845–3864. https://doi.org/10.1016/j.gca.2008.04.038

Andrews-Hanna, J. C., Zuber, M. T., Arvidson, R. E., & Wiseman, S. M. (2010). Early Mars hydrology: Meridiani playa deposits and the sedimentary record of Arabia Terra. *Journal of Geophysical Research*, *115*, E06002. https://doi.org/10.1029/2009JE003485

Arvidson, R. E., Anderson, R. C., Bartlett, P., Bell, J. F. III, Christensen, P. R., Chu, P., et al. (2004). Localization and physical property experiments conducted by opportunity at Meridiani Planum. *Science*, *306*(5702), 1730–1733. https://doi.org/10.1126/science.1104211

Arvidson, R. E., Squyres, S. W., Anderson, R. C., Bell, J. F. III, Blaney, D., Brückner, J., et al. (2006). Overview of the Spirit Mars Exploration Rover mission to Gusev crater: Landing site to backstay rock in the Columbia Hills. *Journal of Geophysical Research*, *111*, E02S01. https://doi.org/10.1029/2005JE002499

Bandfield, J. L., Edwards, C. S., Montgomery, D. R., & Brand, B. D. (2013). The dual nature of the martian crust: Young lavas and old classic materials. *Icarus*, *222*(1), 188–199. https://doi.org/10.1016/j.icarus.2012.10.023

Barlow, N. G. (1995). The degradation of impact craters in Maja Valles and Arabia, Mars. *Journal of Geophysical Research*, *100*(E11), 23307–23,316. https://doi.org/10.1029/95JE02492

Barnhart, C. J., Howard, A. D., & Moore, J. M. (2009). Long-term precipitation and late-stage valley network formation: Landform simulations of Parana Basin, Mars. *Journal of Geophysical Research*, *114*, E01003. https://doi.org/10.1029/2008JE003122

Ben-Hur, M., & Lado, M. (2008). Effect of soil wetting conditions on seal formation, runoff, and soil loss in arid and semiarid soils—A review. *Soil Research*, *46*(3), 191–202. https://doi.org/10.1071/sr07168

Bishop, J. L., Tirsch, D., Tornabene, L. L., Jaumann, R., McEwen, A. S., McGuire, P. C., et al. (2013). Mineralogy and morphology of geologic units at Libya Montes, Mars: Ancient aqueously derived outcrops, mafic flows, fluvial features, and impacts. *Journal of Geophysical Research: Planets*, *118*, 487–513. https://doi.org/10.1029/2012JE004151

Blair, T. C., & McPherson, J. G. (2009). Processes and forms of alluvial fans. In A. J. Parsons, & A. D. Abrahams (Eds.), *Geomorphology of desert environments*, (pp. 413–467). Dordrecht: Springer. https://doi.org/10.1007/978-1-4020-5719-9_14

Braun, J. (2018). A review of numerical modeling studies of passive margin escarpments leading to a new analytical expression for the rate of escarpment migration velocity. *Gondwana Research*, *53*, 209–224. https://doi.org/10.1016/j.gr.2017.04.012

Bridges, N. T., Spagnuolo, M. G., de Silva, S. L., Zimbelman, J. R., & Neely, E. M. (2015). Formation of gravel-mantled megaripples on Earth and Mars: Insights from the Argentinean Puna and wind tunnel experiments. *Journal of Aeolian Research*, *17*, 49–60. https://doi.org/10.1016/j.aeolia.2015.01.007

Carr, M. H. (1981). *The Surface of Mars*. New Haven, CT: Yale University Press.

Carr, M. H. (1995). The Martian drainage system and the origin of valley networks and fretted channels. *Journal of Geophysical Research*, *100*(E4), 7479–7507. https://doi.org/10.1029/95JE00260

Cerdà, A., & García-Fayos, P. (1997). The influence of slope angle on sediment, water and seed losses on badland landscapes. *Geomorphology*, *18*(2), 77–90. https://doi.org/10.1016/s0169-555x(96)00019-0

Channing, A., & Butler, I. B. (2007). Cryogenic opal-A deposition from Yellowstone hot springs. *Earth and Planetary Science Letters*, *257*(1-2), 121–131. https://doi.org/10.1016/j.epsl.2007.02.026

Chapman, C., Pollack, J., & Sagan, C. (1969). An analysis of the Mariner 4 cratering statistics. *The Astronomical Journal*, *74*, 1039–1051. https://doi.org/10.1086/110901

Chapman, C. R. (1974). Cratering on Mars I. Cratering and obliteration history. *Icarus*, *22*(3), 272–291. https://doi.org/10.1016/0019-1035(74)90177-8

Chemtob, S. M., Nickerson, R. D., Morris, R. V., Agresti, D. G., & Catalano, J. G. (2017). Oxidative alteration of ferrous smectites and implications for the redox evolution of early Mars. *Journal of Geophysical Research: Planets*, *122*, 2469–2488. https://doi.org/10.1002/2017JE005331

Cintala, M. J., Head, J. W., & Mutch, T. A. (1976). Craters on the Moon, Mars, and Mercury: A comparison of depth/diameter characteristics. In 7th Lunar Science Conference (pp. 149–151). Houston, TX: Lunar Science Institute.

Clifford, S. M. (1997). The origin of the Martian intercrater plains: The role of liquefaction from impact and tectonic-induced seismicity. In *28th Lunar and Planetary Science Conference* (pp. 241). Houston, TX: Lunar and Planetary Institute.

Cooke, R., Warren, A., & Goudie, A. (~~1993~~). *Desert geomorphology*. London: Taylor & Francis. Q12

Cooke, R. U. (1970). Stone pavements in deserts 1. *Annals of the Association of American Geographers*, *60*(3), 560–577. https://doi.org/10.1111/j.1467-8306.1970.tb00741.x

Craddock, R. A., Bandeira, L., & Howard, A. D. (2018). An assessment of regional variations in Martian modified impact crater morphology. *Journal of Geophysical Research: Planets*, *123*, 763–779. https://doi.org/10.1002/2017JE005412

Craddock, R. A., & Howard, A. D. (2000). Simulated degradation of lunar impact craters and a new method for age dating farside mare deposits. *Journal of Geophysical Research*, *105*(E8), 20387–20401. https://doi.org/10.1029/1999JE001099

Craddock, R. A., & Howard, A. D. (2002). The case for rainfall on a warm, wet early Mars. *Journal of Geophysical Research*, *107*(E11), 5111. https://doi.org/10.1029/2001JE001505

Craddock, R. A., & Lorenz, R. D. (2017). The changing nature of rainfall during the early history of Mars. *Icarus*, *293*, 172–179. https://doi.org/10.1016/j.icarus.2017.04.013

Craddock, R. A., & Maxwell, T. A. (1990). Resurfacing of the Martian highlands in the Amenthes and Tyrrhena region. *Journal of Geophysical Research*, *95*(B9), 14265–14,278. https://doi.org/10.1029/JB095iB09p14265

Craddock, R. A., & Maxwell, T. A. (1993). Geomorphic evolution of the Martian highlands through ancient fluvial processes. *Journal of Geophysical Research*, *98*(E2), 3453–3468. https://doi.org/10.1029/92JE02508

Craddock, R. A., Maxwell, T. A., & Howard, A. D. (1997). Crater morphometry and modification in the Sinus Sabaeus and Margaritifer Sinus regions of Mars. *Journal of Geophysical Research*, *102*(E6), 13321–13340. https://doi.org/10.1029/97JE01084

~~Crumpler, L. S., Arvidson, R. E., Bell, J., Clark, B. C., Cohen, B. A., Farrand, W. H., et al. (2015). Context of ancient aqueous environments on Mars from in situ geologic mapping at Endeavour crater. *Journal of Geophysical Research: Planets*, *120*, 538–569. https://doi.org/10.1002/2014JE004699~~

Crumpler, L. S., & Tanaka, K. L. (2003). Geology and MER target site characteristics along the southern rim of Isidis Planitia, Mars. *Journal of Geophysical Research*, *108*(E12), 8080. https://doi.org/10.1029/2002JE002040

Daly, R. A. (1899). The peneplain—A review. *The American Naturalist*, *33*(386), 127–138. https://doi.org/10.1086/277143

Davis, W. M. (1889). The rivers and valleys of Pennsylvania. *National Geographic Magazine*, *1*(3), 183–253.

Davis, W. M. (1899). The geographical cycle. *Geographical Journal*, *14*(5), 481–504. http://www.jstor.org/stable/1774538. https://doi.org/10.2307/1774538

Dehouck, E., Gaudin, A., Mangold, N., Lajaunie, L., Dauzères, A., Grauby, O., & Le Menn, E. (2014). Weathering of olivine under CO_2 atmosphere: A Martian perspective. *Geochimica et Cosmochimica Acta*, *135*, 170–189. https://doi.org/10.1016/j.gca.2014.03.032

Dohrenwend, J. C., & Parsons, A. J. (2009). Pediments in arid environments. In A. J. Parsons, & A. D. Abrahams (Eds.), *Geomorphology of desert environments*, (pp. 377–411). Dordrecht: Springer. https://doi.org/10.1007/978-1-4020-5719-9_13

Edwards, C. S., Bandfield, J. L., Christensen, P. R., & Rogers, A. D. (2014). The formation of infilled craters on Mars: Evidence for widespread impact induced decompression of the early Martian mantle? *Icarus*, *228*, 149–166. https://doi.org/10.1016/j.icarus.2013.10.005

Edwards, C. S., Nowicki, K. J., Christensen, P. R., Hill, J., Gorelick, N., & Murray, K. (2011). Mosaicking of global planetary image datasets: 1. Techniques and data processing for Thermal Emission Imaging System (THEMIS) multi-spectral data. *Journal of Geophysical Research*, *116*, E10008. https://doi.org/10.1029/2010JE003755

Eggleton, R. A., Foudoulis, C., & Varkevisser, D. (1987). Weathering of basalt: Changes in rock chemistry and mineralogy. *Clays and Clay Minerals*, *35*(3), 161–169. https://doi.org/10.1346/CCMN.1987.0350301

Erkeling, G., Reiss, D., Hiesinger, H., & Jaumann, R. (2010). Morphologic, stratigraphic and morphometric investigations of valley networks in eastern Libya Montes, Mars: Implications for Noachian/Hesperian climate change. *Earth and Planetary Science Letters*, *294*(3-4), 291–305. https://doi.org/10.1016/j.epsl.2009.08.008

Fairén, A. G. (2010). A cold and wet Mars. *Icarus*, *208*(1), 165–175. https://doi.org/10.1016/j.icarus.2010.01.006

Fassett, C. I., & Head, J. W. (2008a). Valley network-fed, open-basin lakes on Mars: Distribution and implications for Noachian surface and subsurface hydrology. *Icarus*, *198*(1), 37–56. https://doi.org/10.1016/j.icarus.2008.06.016

Fassett, C. I., & Head, J. W. (2008b). The timing of Martian valley network activity: Constraints from buffered crater counting. *Icarus*, *195*(1), 61–89. https://doi.org/10.1016/j.icarus.2007.12.009

Forsberg-Taylor, N. K., Howard, A. D., & Craddock, R. A. (2004). Crater degradation in the Martian highlands: Morphometric analysis of the Sinus Sabaeus region and simulation modeling suggest fluvial processes. *Journal of Geophysical Research*, *109*, E05002. https://doi.org/10.1029/2004JE002242

Frey, H. V. (2006). Impact constraints on, and a chronology for, major events in early Mars history. *Journal of Geophysical Research*, *111*, E08S91. https://doi.org/10.1029/2005JE002449

Glotch, T. D., Bandfield, J. L., Tornabene, L. L., Jensen, H. B., & Seelos, F. P. (2010). Distribution and formation of chlorides and phyllosilicates in Terra Sirenum, Mars. *Geophysical Research Letters*, *37*, L16202. https://doi.org/10.1029/2010GL044557

Golombek, M. P., Grant, J. A., Crumpler, L. S., Greeley, R., Arvidson, R. E., Bell, J. F. III, et al. (2006). Erosion rates at the Mars Exploration Rover landing sites and long-term climate change on Mars. *Journal of Geophysical Research*, *111*, E12S10. https://doi.org/10.1029/2006JE002754

Goudge, T. A., Mustard, J. F., Head, J. W., & Fassett, C. I. (2012). Constraints on the history of open-basin lakes on Mars from the composition and timing of volcanic resurfacing. *Journal of Geophysical Research*, *117*, E00J21. https://doi.org/10.1029/2012JE004115

Graham, D. H., & Cawley, J. C. (2017). Alkali silica reactivity a problem on Earth, a solution on Mars. In 48^{th} *Lunar and Planetary Science Conference*, abstract 2209. Houston, TX: Lunar and Planetary Institute.

Grant, J. A., & Schultz, P. H. (1993). Degradation of selected terrestrial and Martian impact craters. *Journal of Geophysical Research*, *98*(E6), 11025–11,042. https://doi.org/10.1029/93JE00121

Hartmann, W. K. (1973). Martian cratering, 4, Mariner 9 initial analysis of cratering chronology. *Journal of Geophysical Research*, *78*(20), 4096–4116. https://doi.org/10.1029/JB078i020p04096

Hartmann, W. K. (2005). Martian cratering 8: Isochron refinement and the chronology of Mars. *Icarus*, *174*(2), 294–320. https://doi.org/10.1016/j.icarus.2004.11.023

Hartmann, W. K., & Neukum, G. (2001). Cratering chronology and the evolution of Mars. *Space Science Reviews*, *12*, 165–194. https://doi.org/10.1007/978-94-017-1035-0_6

Heimsath, A. M., Chappell, J., Finkel, R. C., Fifield, K., & Alimanovic, A. (2006). Escarpment erosion and landscape evolution in southeastern Australia. In S. D. Willett, N. Hovius, M. T. Brandon, & D. M. Fisher (Eds.), *Tectonics, climate, and landscape evolution*, *Geological Society of America Special Paper*, (Vol. 398, pp. 173–190). https://doi.org/10.1130/2006.2398(10

Howard, A. D. (2007). Simulating the development of Martian highland landscapes through the interaction of impact cratering, fluvial erosion, and variable hydrologic forcing. *Geomorphology*, *91*(3-4), 332–363. https://doi.org/10.1016/j.geomorph.2007.04.017

Howard, A. D., Breton, S., & Moore, J. M. (2016). Formation of gravel pavements during fluvial erosion as an explanation for persistence of ancient cratered terrain on Titan and Mars. *Icarus*, *270*, 100–113. https://doi.org/10.1016/j.icarus.2015.05.034

Howard, A. D., Moore, J. M., & Irwin, R. P. (2005). An intense terminal epoch of widespread fluvial activity on early Mars: 1. Valley network incision and associated deposits. *Journal of Geophysical Research*, *110*, E12S14. https://doi.org/10.1029/2005JE002459

Hynek, B. M., Beach, M., & Hoke, M. R. (2010). Updated global map of Martian valley networks and implications for climate and hydrologic processes. *Journal of Geophysical Research*, *115*, E09008. https://doi.org/10.1029/2009JE003548

Irwin, R. P. III, Craddock, R. A., & Howard, A. D. (2005). Interior channels in Martian valley networks: Discharge and runoff production. *Geology*, *33*(6), 489–492. https://doi.org/10.1130/g21333.1

Irwin, R. P. III, Craddock, R. A., Howard, A. D., & Flemming, H. L. (2011). Topographic influences on development of Martian valley networks. *Journal of Geophysical Research*, *116*, E02005. https://doi.org/10.1029/2010JE003620

Irwin, R. P. III, Lewis, K. W., Howard, A. D., & Grant, J. A. (2015). Paleohydrology of Eberswalde crater, Mars. *Geomorphology*, *240*, 83–101. https://doi.org/10.1016/j.geomorph.2014.10.012

Irwin, R. P. III, Tanaka, K. L., & Robbins, S. J. (2013). Distribution of Early, Middle, and Late Noachian cratered surfaces in the Martian highlands: Implications for resurfacing events and processes. *Journal of Geophysical Research: Planets*, *118*, 278–291. https://doi.org/10.1002/jgre.20053

Irwin, R. P. III, & Watters, T. R. (2010). Geology of the Martian crustal dichotomy boundary: Age, modifications, and implications for modeling efforts. *Journal of Geophysical Research*, *115*, E11006. https://doi.org/10.1029/2010JE003658

Irwin, R. P. III, Wray, J. J., Mest, S. C., & Maxwell, T. A. (2018). Wind-eroded crater floors and intercrater plains, Terra Sabaea, Mars. *Journal of Geophysical Research: Planets*, *123*, 445–467. https://doi.org/10.1002/2017JE005270

Jankowski, D. G., & Squyres, S. W. (1992). The topography of impact craters in "softened" terrain on Mars. *Icarus*, *100*(1), 26–39. https://doi.org/10.1016/0019-1035(92)90015-Y

Jaumann, R., Nass, A., Tirsch, D., Reiss, D., & Neukum, G. (2010). The western Libya Montes valley system on Mars: Evidence for episodic and multi-genetic erosion events during the Martian history. *Earth and Planetary Science Letters*, *294*(3-4), 272–290. https://doi.org/10.1016/j.epsl.2009.09.026

Jones, K. L. (1974). Evidence for an episode of Martian crater obliteration intermediate in Martian history. *Journal of Geophysical Research*, *79*(26), 3917–3931. https://doi.org/10.1029/JB079i026p03917

Kite, E. S., Lewis, K. W., Lamb, M. P., Newman, C. E., & Richardson, M. I. (2013). Growth and form of the mound in Gale crater, Mars: Slope wind enhanced erosion and transport. *Geology*, *41*(5), 543–546. https://doi.org/10.1130/G33909.1

Kreslavsky, M. A., & Head, J. W. (2003). North-south topographic slope asymmetry on Mars: Evidence for insolation-related erosion at high obliquity. *Geophysical Research Letters*, *30*(15), 1815. https://doi.org/10.1029/2003GL017795

Kreslavsky, M. A., & Head, J. W. (2018). Mars climate history: Insights from impact crater wall slope statistics. *Geophysical Research Letters*, *45*, 1751–1758. https://doi.org/10.1002/2017GL075663

Landis, G. A., Blaney, D., Cabrol, N., Clark, B. C., Farmer, J., Grotzinger, J., et al.; Mer Athena Science Team (2004). Transient liquid water as a mechanism for induration of soil crusts on Mars. In *35th Lunar and Planetary Science Conference*, abstract 2188. Houston, TX: Lunar and Planetary Institute.

Leake, M. A. (1982). The intercrater plains of Mercury and the Moon: Their nature, origin, and role in terrestrial planet evolution (Doctoral dissertation). Tucson, AZ: University of Arizona. In *Advances in Planetary Geology*, pp. 1–535, NASA Technical Memorandum 84894.

Malin, M. C. (1976), Nature and origin of intercrater plains on Mars. In *Studies of the surface morphology of Mars* (Ph.D. dissertation). Retrieved from https://thesis.library.caltech.edu/4435/1/Malin_mc_1976.pdf. Pasadena, CA: California Institute of Technology.

Malin, M. C., & Dzurisin, D. (1977). Landform degradation on Mercury, the Moon, and Mars: Evidence from crater depth/diameter relationships. *Journal of Geophysical Research*, *82*(2), 376–388. https://doi.org/10.1029/JB082i002p00376

Malin, M. C., & Edgett, K. S. (2000). Sedimentary rocks of early Mars. *Science*, *290*(5498), 1927–1937. https://doi.org/10.1126/science.290.5498.1927

Malin, M. C., & Edgett, K. S. (2001). Mars Global Surveyor Mars Orbiter Camera: Interplanetary cruise through primary mission. *Journal of Geophysical Research*, *106*(E10), 23429–23570. https://doi.org/10.1029/2000JE001455

Malin, M. C., & Edgett, K. S. (2003). Evidence for persistent flow and aqueous sedimentation on early Mars. *Science*, *302*(5652), 1931–1934. https://doi.org/10.1126/science.1090544

Mangold, N., Adeli, S., Conway, S., Ansan, V., & Langlais, B. (2012). A chronology of early Mars climatic evolution from impact crater degradation. *Journal of Geophysical Research*, *117*, E04003. https://doi.org/10.1029/2011JE004005

Matsubara, Y., & Howard, A. D. (2009). A spatially explicit model of runoff, evaporation, and lake extent: Application to modern and late Pleistocene lakes in the Great Basin region, western United States. *Water Resources Research*, *45*, WO6435. https://doi.org/10.1029/2007WR005953

Matsubara, Y., Howard, A. D., & Gochenour, J. P. (2013). Hydrology of early Mars: Valley network incision. *Journal of Geophysical Research: Planets*, *118*, 1365–1387. https://doi.org/10.1002/jgre.20081

Matsubara, Y., Howard, A. D., & Irwin, R. P. III (2018). Constraints on the Noachian paleoclimate of the Martian highlands from landscape evolution modeling. *Journal of Geophysical Research: Planets*. https://doi.org/10.1029/2018JE005572 Q13

McCoy, T. J., Sims, M., Schmidt, M. E., Edwards, L., Tornabene, L. L., Crumpler, L. S., et al. (2008). Structure, stratigraphy, and origin of Husband Hill, Columbia Hills, Gusev crater, Mars. *Journal of Geophysical Research*, *113*, E06S03. https://doi.org/10.1029/2007JE003041

McLennan, S. M. (2003). Sedimentary silica on Mars. *Geology*, *31*(4), 315–318. https://doi.org/10.1130/0091-7613(2003)031<0315:SSOM>2.0.CO;2

Migoń, P. (2004). Planation surface. In A. S. Goudie (Ed.), *Encyclopedia of geomorphology*, (pp. 788–792). London: Routledge.

Milliken, R. E., Swayze, G. A., Arvidson, R. E., Bishop, J. L., Clark, R. N., Ehlmann, B. L., et al. (2008). Opaline silica in young deposits on Mars. *Geology*, *36*(11), 847–850. https://doi.org/10.1130/g24967a.1

Mittlefehldt, D. W., Gellert, R., vanBommel, S., Ming, D. W., Yen, A. S., Clark, B. C., et al. (2018). Diverse lithologies and alteration events on the rim of Noachian-aged Endeavour crater, Meridiani Planum, Mars: In situ compositional evidence. *Journal of Geophysical Research: Planets*, *123*, 1255–1306. https://doi.org/10.1002/2017JE005474

Moore, J. M., & Howard, A. D. (2005). Large alluvial fans on Mars. *Journal of Geophysical Research*, *110*, E04005. https://doi.org/10.1029/2004JE002352

Murchie, S. L., Seelos, F. P. IV, Hash, C. D., Humm, D. C., Malaret, E., McGovern, J. A., et al. (2009). Compact reconnaissance imaging spectrometer for Mars investigation and data set from the Mars Reconnaissance Orbiter's primary science phase. *Journal of Geophysical Research*, *114*, E00D07. https://doi.org/10.1029/2009JE003344

Murray, B. C., Soderblom, L. A., Sharp, R. P., & Cutts, J. A. (1971). The surface of Mars 1. Cratered terrains. *Journal of Geophysical Research*, *76*(2), 313–330. https://doi.org/10.1029/jb076i002p00313

Oberbeck, V. R., Quaide, W. L., Arvidson, R. E., & Aggarwal, H. R. (1977). Comparative studies of lunar, Martian, and Mercurian craters and plains. *Journal of Geophysical Research*, *82*(11), 1681–1698. https://doi.org/10.1029/jb082i011p01681

Parsons, A. J., Abrahams, A. D., & Howard, A. D. (2009). Rock-mantled slopes. In A. J. Parsons, & A. D. Abrahams (Eds.), *Geomorphology of desert environments*, (pp. 233–263). Dordrecht: Springer. https://doi.org/10.1007/978-1-4020-5719-9_9

Perry, R. S., Lynne, B. Y., Sephton, M. A., Kolb, V. M., Perry, C. C., & Staley, J. T. (2006). Baking black opal in the desert sun: The importance of silica in desert varnish. *Geology*, *34*(7), 537–540. https://doi.org/10.1130/g22352a.1

Phillips, J. (1995). Nonlinear dynamics and the evolution of relief. *Geomorphology*, *14*(1), 57–64. https://doi.org/10.1016/0169-555x(95)00026-2

Phillips, R. J., Zuber, M. T., Solomon, S. C., Golombek, M. P., Jakosky, B. M., Banerdt, W. B., et al. (2001). Ancient geodynamics and global-scale hydrology on Mars. *Science*, *291*(5513), 2587–2591. https://doi.org/10.1126/science.1058701

Pieri, D. C. (1980). Geomorphology of Martian valleys (Doctoral dissertation). Ithaca, NY: Cornell University. In *Advances in Planetary Geology*, pp. 1–160, NASA Technical Memorandum 81979.

Ritter, D. F. (1988). Landscape analysis and the search for geomorphic unity. *Geological Society of America Bulletin*, *100*(2), 160–171. https://doi.org/10.1130/0016-7606(1988)100<0160:LAATSF<2.3.CO;2

Ritter, D. F., Kochel, R. C., & Miller, J. R. (2011). *Process geomorphology*, (Fifth ed.). Long Grove, IL: Waveland Press Inc.

Robbins, S. J., & Hynek, B. M. (2012a). A new global database of Mars impact craters ≥ 1 km: 1. Database creation, properties, and parameters. *Journal of Geophysical Research*, *117*, E05004. https://doi.org/10.1029/2011JE003966

10.1029/2018JE005681

Robbins, S. J., & Hynek, B. M. (2012b). A new global database of Mars impact craters $\geq$ 1 km: 2. Global crater properties and regional variations of the simple-to-complex transition diameter. *Journal of Geophysical Research*, *117*, E06001. https://doi.org/10.1029/2011JE003967

Rogers, A. D., Warner, N. H., Golombek, M. P., Head, J. W. III, & Cowart, J. C. (2018). Areally extensive surface bedrock exposures on Mars: Many are clastic rocks, not lavas. *Geophysical Research Letters*, *45*, 1767–1777. https://doi.org/10.1002/2018GL077030

Salvatore, M. R., Mustard, J. F., Head, J. W., Cooper, R. F., Marchant, D. R., & Wyatt, M. B. (2013). Development of alteration rinds by oxidative weathering processes in Beacon Valley, Antarctica, and implications for Mars. *Geochimica et Cosmochimica Acta*, *115*, 137–161. https://doi.org/10.1016/j.gca.2013.04.002

Schumm, S. A. (1973). Geomorphic thresholds and complex response of drainage systems. In M. Morisawa (Ed.), *Fluvial geomorphology*, *Publications in geomorphology*, (pp. 299–310). Binghamton, NY: State University of New York.

Scott, D. H., & Carr M. H. (1978). Geologic map of Mars (Geologic Investigations Series Map I-1083). Reston, VA: U.S. Geological Survey.

Scott, D. H., Tanaka, K. L., Greeley, R., & Guest, J. E. (1986–1987). Geologic map of the western equatorial, eastern equatorial, and polar regions of Mars (*Miscellaneous Investigations Series Maps I-1802-A, I-1802-B, and I-1802-C*). Reston, VA: U.S. Geological Survey.

Selby, M. J. (1993). *Hillslope materials and processes*, (2nd ed.). Oxford, UK: Oxford Univ. Press.

Sharp, R. P. (1968). Surface processes modifying Martian craters. *Icarus*, *8*(1–3), 472–480. https://doi.org/10.1016/0019-1035(68)90093-6

Smith, D. E., Zuber, M. T., Neumann, G. A., Guinness, E. A., & Slavney, S. (2003). Mars Global Surveyor laser altimeter mission experiment gridded data record, MGS-M-MOLA-5-MEGDR-L3-V1.0, NASA Planetary Data System.

Smith, D. E., Zuber, M. T., Solomon, S. C., Phillips, R. J., Head, J. W., Garvin, J. B., et al. (1999). The global topography of Mars and implications for surface evolution. *Science*, *284*(5419), 1495–1503. https://doi.org/10.1126/science.284.5419.1495

Soderblom, L. A., Anderson, R. C., Arvidson, R. E., Bell, J. F. III, Cabrol, N. A., Calvin, W., et al. (2004). Soils of Eagle crater and Meridiani Planum at the Opportunity rover landing site. *Science*, *306*(5702), 1723–1726. https://doi.org/10.1126/science.1105127

Solomon, S. C. (1978). On volcanism and thermal tectonics on one-plate planets. *Geophysical Research Letters*, *5*(6), 461–464. https://doi.org/10.1029/gl005i006p00461

Squyres, S. W., Arvidson, R. E., Blaney, D. L., Clark, B. C., Crumpler, L., Farrand, W. H., et al. (2006). Rocks of the Columbia Hills. *Journal of Geophysical Research*, *111*, E02S11. https://doi.org/10.1029/2005JE002562

Stoertz, G. E., & Ericksen, G. E. (1974). Geology of salars in northern Chile. Professional Paper 811. Reston, VA: U. S. Geological Survey.

Strudley, M. W., Murray, A. B., & Haff, P. K. (2006). Regolith thickness instability and the formation of tors in arid environments. *Journal of Geophysical Research*, *111*, F03010. https://doi.org/10.1029/2005JF000405

Tanaka, K. L. (1986). The stratigraphy of Mars. *Journal of Geophysical Research*, *91*(B13), E139. https://doi.org/10.1029/jb091ib13p0e139

Tanaka, K. L., Isbell, N. K., Scott, D. H., Greeley, R., & Guest, J. E. (1988). The resurfacing history of Mars: A synthesis of digitized, Viking-based geology. In G. Ryder (Ed.), *Proceedings of the 18^{th} Lunar and Planetary Science Conference*, (pp. 665–678). Cambridge, UK: Cambridge University Press and Houston, TX: Lunar and Planetary Institute.

Tanaka, K. L., Skinner Jr., J. A., Dohm, J. M., Irwin III, R. P., Kolb, E. J., Fortezzo, C. M., et al. (2014). Geologic map of Mars (*Scientific Investigations Map I-3292*). Reston, VA: U.S. Geological Survey. https://dx.doi.org/10.3133/sim3292

Thiagarajan, N., & Lee, C. T. A. (2004). Trace-element evidence for the origin of desert varnish by direct aqueous atmospheric deposition. *Earth and Planetary Science Letters*, *224*(1-2), 131–141. https://doi.org/10.1016/j.epsl.2004.04.038

Tornabene, L. L., Moersch, J. E., McSween, H. Y. Jr., Hamilton, V. E., Piatek, J. L., & Christensen, P. R. (2008). Surface and crater-exposed lithologic units of the Isidis Basin as mapped by coanalysis of THEMIS and TES derived data products. *Journal of Geophysical Research*, *113*, E10001. https://doi.org/10.1029/2007JE002988

Tosca, N. J., McLennan, S. M., Lindsley, D. H., & Schoonen, M. A. A. (2004). Acid-sulfate weathering of synthetic Martian basalt: The acid fog model revisited. *Journal of Geophysical Research*, *109*, E05003. https://doi.org/10.1029/2003JE002218

Twidale, C. R. (2002). The two-stage concept of landform and landscape development involving etching: Origin, development and implications of an idea. *Earth-Science Reviews*, *57*(1-2), 37–74. https://doi.org/10.1016/S0012-8252(01)00059-9

Twidale, C. R. (2014). Pediments and platforms: Problems and solutions. *Géomorphologie: Relief, Processus, Environnement*, *20*(1), 43–56. https://doi.org/10.4000/geomorphologie.10480

United Nations Educational, Scientific and Cultural Organization (UNESCO) (1979). Map of the world distribution of arid regions, explanatory note. *Programme on Man and the Biosphere (MAB) Technical Notes 7*. Paris: UNESCO.

Watters, T. R., McGovern, P. J., & Irwin, R. P. III (2007). Hemispheres apart: The crustal dichotomy on Mars. *Annual Review of Earth and Planetary Sciences*, *35*(1), 621–652. https://doi.org/10.1146/annurev.earth.35.031306.140220

Wells, S. G., McFadden, L. D., Poths, J., & Olinger, C. T. (1995). Cosmogenic ^{3}He surface-exposure dating of stone pavements: Implications for landscape evolution in deserts. *Geology*, *23*(7), 613–616. https://doi.org/10.1130/0091-7613(1995)023<0613:CHSEDO>2.3.CO;2

Werner, S. C. (2008). The early martian evolution—Constraints from basin formation ages. *Icarus*, *195*(1), 45–60. https://doi.org/10.1016/j.icarus.2007.12.008

Werner, S. C., & Tanaka, K. L. (2011). Redefinition of the crater-density and absolute-age boundaries for the chronostratigraphic system of Mars. *Icarus*, *215*(2), 603–607. https://doi.org/10.1016/j.icarus.2011.07.024

Wichman, R. W., & Schultz, P. H. (1989). Sequence and mechanisms of deformation around the Hellas and Isidis impact basins on Mars. *Journal of Geophysical Research*, *94*(B12), 17333–17,357. https://doi.org/10.1029/JB094iB12p17333

Wilhelms, D. E. (1974). Comparison of Martian and lunar geologic provinces. *Journal of Geophysical Research*, *79*(26), 3933–3941. https://doi.org/10.1029/jb079i026p03933

Wohl, E. (2000). *Mountain rivers*, *Water Resources Monograph*, (Vol. 14). Washington, DC: American Geophysical Union.

Wolman, M. G., & Miller, J. P. (1960). Magnitude and frequency of forces in geomorphic processes. *Journal of Geology*, *68*(1), 54–74. https://doi.org/10.1086/626637.